Journal of Renewable Energy and Sustainable Development (RESD) Volume 11, Issue 2, December 2025 - ISSN 2356-8569
http://dx.doi.org/10.21622/RESD.2025.11.2.1279

Received: 27 March 2025 Accepted: 25 July 2025 Published: 31 August 2025

Super Capacitor-Enhanced Neural Control (SENCO) for Power Quality Optimization in Wind Turbine-Integrated Microgrids

Rutuja S. Hiware [1*], and P. M. Daigavane [2]

[1*,2] G H Raisoni University, Department of Electrical Engineering, Anjangaon Bari Road, Amravati, Maharashtra, India

rutujahiware9987@gmail.com, pdaigavane@gmail.com

Abstract

Wind-integrated micro grids face significant challenges in voltage stability, power flow regulation, and system reliability due to the highly variable and intermittent nature of wind energy. Traditional Unified Power Quality Conditioners (UPQCs), while effective in mitigating certain power quality issues, lack inherent energy storage capability, limiting their performance during sudden supply-demand imbalances. To address this limitation, a Super Capacitor-Enhanced Neural Control (SENCO) system is proposed, which integrates a high-speed super capacitor module into the UPQC. The super capacitor provides immediate energy buffering during transient disturbances, enabling rapid compensation for voltage sags, frequency deviations, and wind power fluctuations. This integration enhances the dynamic response and ride-through capability of the UPQC, making it more effective in stabilizing renewable-based microgrids. An Artificial Neural Network (ANN)-based Pulse Width Modulation (PWM) control is employed to adaptively manage the system under varying conditions. Optimization algorithms are further applied to improve operational efficiency. The proposed SENCO system thus addresses a key deficiency in conventional UPQCs by enabling energy-aware compensation, offering a robust solution for maintaining power quality and grid stability in renewable-rich microgrid environments.

Index-words: *Super Capacitor-Enhanced Neural Control, Unified Power Quality Conditioners, Artificial Neural Network, Pulse Width Modulation, Total Harmonic Distortion.*

Table 1: List of Symbols

S.No	Symbols	Function	S.No	Symbols	Function
1	P_r	Real power at the rotor side	11	I_d	d-axis component of current in rotating reference frame
2	v_{dr}	d-axis component of the rotor voltage	12	I_q	q-axis component of current in rotating reference frame
3	v_{qr}	q-axis component of the rotor voltage	14	I_o	Zero-sequence component of current
4	i_{dr}	d-axis component of the rotor current	15	$\emptyset_p$	Difference in phase between the positive-sequence component and the reference voltage.
5	i_{qr}	q-axis component of the rotor current	16	θ_d	Rotating frame angle
6	P_s	Real power at the Stator side	17	ω_d	Angular velocity
7	v_{ds}	d-axis component of the Stator side	18	$\frac{dv}{dt}$	Rate of change of voltage across the storage system
8	v_{qs}	q-axis component of the Stator side	19	$\emptyset_0$	Phase angle of zero-sequence voltage
9	i_{ds}	d-axis component of the stator voltage	20	E	stored energy
10	i_{qs}	q-axis component of the stator voltage	21	$P_{generated}$	power generated by the turbine
11	P_{loss}	Power losses in the system.	22	C	capacitance of a supercapacitor
12	P_{stored}	power drawn from the ESS	23	V	voltage across the capacitor
13	P_{load}	power consumed by the loads in the microgrids	24	u'_d	Reference voltage

Volume 11, Issue 2, December 2025 - ISSN 2356-8569
http://dx.doi.org/10.21622/RESD.2025.11.2.1279

I. Introduction

The growing demand for electricity and increasing environmental concerns have accelerated the integration of renewable energy sources such as solar and wind into modern power systems. Among these, wind energy plays a pivotal role due to its availability and scalability. However, the inherent intermittency and variability of wind energy introduce several challenges in maintaining power quality (PQ), including voltage fluctuations, harmonics, flicker, and frequency deviations [1]. These issues necessitate advanced power management strategies to ensure stable and reliable operation in grid-connected systems. Power quality is a critical aspect in evaluating the compatibility of energy sources with existing infrastructure. According to IEEE Std. 1100TM-2005, power quality refers to the reliable supply of voltage and grounding conditions that support the proper operation of sensitive equipment [2]. A high-quality electrical supply is characterized by a nearly sinusoidal voltage waveform at the rated frequency and magnitude. To standardize PQ performance, international bodies such as the International Electrotechnical Commission (IEC) have established regulatory limits for various parameters in grid-connected renewable energy systems. Grid strength, defined by its short-circuit capacity and impedance characteristics, significantly influences the ability to mitigate PQ disturbances and maintain system stability [3].

Flexible AC Transmission Systems (FACTS) devices are widely used to address PQ and overload issues in renewable energy applications. These compensators are generally classified as series and shunt types. Series devices such as the Dynamic Voltage Restorer (DVR) and Static Synchronous Series Compensator (SSSC) are primarily employed for voltage regulation, while shunt devices like DSTATCOM, STATCOM, and Thyristor-Controlled Reactors (TCR) are used to compensate for reactive power and voltage imbalances [4]. The strategic placement and coordinated control of these devices are essential for enhancing network performance and optimizing power delivery infrastructure [5]. The Unified Power Quality Conditioner (UPQC), a combination of series and shunt active filters, has emerged as a comprehensive solution for mitigating both voltage and current-related PQ issues in microgrid environments [6]. Its performance, however, is heavily dependent on the control strategy employed to adapt to dynamic operating conditions. In this context, the integration of energy storage systems such as supercapacitors offers significant advantages. Super capacitors—also known as ultra-capacitors—exhibit high power density, rapid charge-discharge capabilities, and a long operational lifecycle. These features make them particularly suitable for handling transient events, such as voltage sags, frequency deviations, and short-term power interruptions in Distributed Renewable Energy Generation Systems (DREGS) and micro grids [7].

In wind-integrated micro grids, the choice of wind energy conversion system (WECS) topology plays a crucial role in determining PQ performance. Grid-tied WECSs can be broadly categorized based on generator type and power electronic interface. Fixed-Speed Induction Generators (FSIG) are cost-effective and robust but lack reactive power control and are highly sensitive to grid disturbances. Variable-Slip Wound Rotor Induction Generators (WRIG) offer limited speed variability and marginally improved controllability. Doubly-Fed Induction Generators (DFIG) allow variable-speed operation and better efficiency through partial-scale converters; however, they are vulnerable to voltage dips and require complex protection schemes. Despite the extensive body of literature on PQ management in renewable-based micro grids, several limitations persist. Most existing works address either voltage or current disturbances in isolation, thereby providing only partial mitigation [8]. Although artificial intelligence (AI) techniques such as Artificial Neural Networks (ANN) and Adaptive Neuro-Fuzzy Inference Systems (ANFIS) [9] have been applied in UPQC control, these approaches are typically implemented uniformly across both the Series Active Filter (SAF) and Parallel Active Filter (PAF), reducing adaptability to dynamic conditions [10]. Furthermore, hybrid control schemes that combine the predictive strength of Model Predictive Control (MPC) with the learning capabilities of ANN remain underexplored [11]. Similarly, the integration of supercapacitor-based energy storage within UPQC systems, especially in wind-integrated microgrids, has not been extensively addressed in current research [12].

This paper aims to bridge these gaps by proposing a novel SENCO-based hybrid control strategy that integrates ANN-driven Pulse Width Modulation (PWM) and super capacitor energy storage within a UPQC framework. The proposed approach is designed to enhance both voltage and current

quality under dynamic grid conditions, thereby ensuring improved stability, efficiency, and resilience of power management in wind turbine-integrated micro grids. The key contributions include:

- **Integration of UPQC for Voltage Stability:** The system incorporates UPQC to maintain stable grid and load voltages under fluctuating wind conditions.
- **Dynamic Compensation for Power Variations:** Utilizes supercapacitors as a short-term energy storage solution to effectively manage power fluctuations caused by wind intermittencies and grid failures.
- **ANN-Based Control:** Implements ANN-based monitoring and control to dynamically adjust network parameters for efficient energy management and enhanced system responsiveness.
- **Mitigation of Harmonic Distortion and Enhanced Stability:** Significantly reduces harmonic distortion in grid and load currents while ensuring stability of key system parameters.

Thus, the proposed model addresses critical challenges such as power quality, voltage stability, and harmonic distortion. The SENCO system emerges as an effective solution, significantly improving power quality and ensuring reliable energy delivery in wind-integrated micro grids. This proposed model the document is structured as follows: *Section 1* presents the study's background, including research objectives and motivation; *Section 2* reviews prior work and highlights the research gap; *Section 3* explains model and techniques developed in Wind Turbine-Integrated Micro grids; *Section 4* interprets findings and compares performance with existing approaches; and *Section 5* summarizes key contributions and future directions. Finally, references provide supporting literature.

II. Literature review

Wang et al. [13] proposed a novel UPQC predictive direct control strategy named Power Angle Control Strategy (PDCS-PAC). By integrating this direct control strategy with Finite Control Set Model Predictive Control (FCS-MPC), they established a simplified control system model in the dq coordinate system. This method aimed to streamline the controller structure and mitigate algorithmic complexity. By examination of the PAC mechanism, they introduced an instantaneous power angle determination method that leveraged reactive power equalization techniques. A predictive direct control strategy was developed for both series and shunt sides of UPQC, accounting for the system's active power balance and maintaining a constant load fundamental voltage amplitude. However, its reliance on predictive direct control introduced additional computational complexity and real-time processing requirements.

Das et al [14] investigated four different control techniques: dq, pq, ANN, and Adaptive Neuro Fuzzy Inference System (ANFIS) in hybrid combinations to control both PAF and SAF in the UPQC device. Four hybrid cases were formulated to tackle three primary power quality problems: *harmonic distortion, voltage sag, and swell*, to evaluate the effectiveness of the control techniques. Results showed that the hybrid ANFIS-ANN control strategy achieved a notable reduction in THD, with THD values of 4.26% for load voltage and 0.08% for source current after compensation, surpassing the performance of other methods. However, the study faced a limitation in determining the optimal control strategy for all scenarios due to the varying effectiveness of the techniques across different system dynamics, operating conditions, and parameter uncertainties.

Lei et al [15] examined a Distributed Generation (DG) system integrating a wind turbine and a photovoltaic (PV) system with a UPQC. This configuration delivered active power to the grid while improving power quality parameters such as voltage fluctuations, harmonics, and power factor (PF). UPQC operated using a dual compensation scheme, where the parallel and series converters functioned as sinusoidal voltage and current sources, enabling seamless transitions between grid-connected and islanded modes without causing disturbances to the load voltage. To manage sudden changes in solar radiation or wind speed, the Feed Forward Control Law (FFCL) was implemented to facilitate faster power balance adjustments by regulating current references for the series converter, thereby improving the dynamic responses of converter currents and DC bus voltage. However, despite the FFCL improving power balance adjustments, variations in environmental

Volume 11, Issue 2, December 2025 - ISSN 2356-8569
http://dx.doi.org/10.21622/RESD.2025.11.2.1279

conditions led to transient disturbances and required additional measures for robust operation.

Dheeban et al [16] examined a UPQC integrated with photovoltaic (PV) systems, incorporating bidirectional shunt and series converters. Control strategies employed a hybrid approach combining Unit Vector Template and p-q theory. The need for improved precision in a closed-loop structure led to the exploration of alternative control methods, as conventional mathematical-based PI controllers were found to be insufficient in managing transient oscillations. Through analysis, the proposed PV-UPQC system was evaluated using an Adaptive Neuro-Fuzzy controller featuring a reinforced learning algorithm. This fuzzy-model-based (FMB) controller improved system performance by leveraging linguistic rules to infer system parameters and assist in referencing the current generation. Application of ANFIS significantly reduced the THD percentage, enhancing the overall efficiency.

Srilakshmi et al [17] focused on designing a UPQC by optimizing the active filter and PID Controller (PIDC) parameters using the enhanced most valuable player algorithm (EMVPA). The main aim was to tackle power quality issues such as voltage distortions and THD in a distribution system that included UPQC, solar, wind, Battery Energy Storage Systems (BESS), and EV (U-SWBEV). Additionally, the study aimed to regulate power flow among Renewable Energy Sources (RES), the grid, EV, BESS, and consumer loads using an ANFIS. This integration ensured a reliable electricity supply, efficient utilization of generated power, and effective fulfillment of demand. The proposed system achieved THD values ranging from 2.26% to 4.5% across four different case studies, with the power factor approaching unity and appropriate power sharing. However, ANFIS models faced challenges in precisely capturing the complex connections between the dynamic behavior of wind turbines and their resulting power output.

Pushkarna et al [18] introduced a compensation technique that employed UPQC to address voltage fluctuations in Wind Farms (WF). A custom control strategy was developed to regulate WF terminal voltages and reduce grid-side voltage fluctuations. This strategy focused on controlling active and reactive power in UPQC's shunt and series converters, along with transmission of power through UPQC DC-Link. Unlike other methods that relied on reactive power, this approach enhanced UPQC's compensation capability. The study evaluated THD performance using a FUZZY controller and compared the outcomes with those obtained from a PI controller.

Jin et al [19] proposed and designed an Interline AC-DC UPQC protection device that incorporated superconducting magnetic energy storage (SMES) to improve low voltage ride-through (LVRT) capability and stabilize power output in hybrid Wind Energy Conversion Systems (WECS) consisting of DFIG. The UPQC's AC side functioned as a DVR, which was connected in series with the DFIG terminal, while the DC side was linked in parallel with the PMSG's DC bus to maintain voltage and adjust power. The research also involved designing a superconducting coil (SC) with specifications of 4.76-H/1760-A as the energy storage component for UPQC functionality.

Mahar et al [20] investigated the integration of a UPQC with a grid-connected microgrid to improve power quality during generation. An ANN controller was proposed for the UPQC's voltage source converter, reducing system complexity and cost by eliminating the need for mathematical translations and expensive controllers such as DSP and FPGA. Nonlinear unbalanced load and harmonic supply voltage were employed to assess the effectiveness of the PV-battery-UPQC system integrated with an ANN-based controller, successfully mitigating voltage issues like sag and swell. An ANN control system, trained using the Levenberg-Marquardt backpropagation algorithm, was utilized to produce accurate reference signals and ensure the stability of DC-link capacitor voltage.

Sivakumar et al [21] introduced an advanced controller to enhance the performance of series and shunt APF and address power quality issues. By combining ANN and Gravitational Search Algorithm (GSA) techniques, the controller was designed to generate control signals for the APFs, effectively reducing power quality problems. The shunt APF was used to mitigate harmonic disturbances, while the enhanced controller regulated the DC link voltage. The study evaluated the THD value to assess the efficacy of the proposed method, which was subsequently implemented and tested.

Yang et al [22] proposed a Dual Active Bridge (DAB)-based DC-UPQC integrated with superconducting magnetic energy storage (SMES) for DC Doubly Fed Induction Generator (DC-DFIG) wind energy conversion systems (WECS). The DC-UPQC featured

http://dx.doi.org/10.21622/RESD.2025.11.2.1279

parallel-side DAB (PDAB), series-side DAB (SDAB), and SMES components, which were used for voltage compensation, current regulation, and energy storage, respectively. The study delved into circuit principles of PDAB and SDAB and provided a model for the SMES system. A DC dual control strategy was introduced to address DC voltage oscillations resulting from AC-side asymmetrical faults. A case study demonstrated the effectiveness of the SMES-based DC-UPQC in high-power applications interfacing with a DC power grid.

Kotla et al [23] discussed the integration of an ultra-capacitor (UC) with a UPQC in Distributed Renewable Energy Generation Systems (DREGS) to ensure power quality during intermittencies. The UC, known for its high power and low energy density, compensated for microgrid (MG) intermittencies. The study addressed control and design aspects of UC, along with a bidirectional converter for UC charging and discharging, and UPQC. The UPQC functioned as a DVR for the MG side and an Active Power Filter (APF) for the load side.

Döşoğlu et al [24] aimed to enhance stator dynamics and rotor dynamic modelling to mitigate oscillations induced by grid faults. Electromotive force models were devised for both rotor and stator dynamics. Additionally, models were developed for coordinating DFIG using a lookup-table-based super capacitor and a decoupled STATCOM. Analyses of three-phase and two-phase faults were conducted using these models. The system demonstrated rapid stabilization and damping of oscillations during various grid faults, facilitated by the developed Low Voltage Ride through (LVRT) models.

Afzal et al [25] examined a supercapacitor energy storage system (SCESS)-based STATCOM for improving power quality in grid-connected photovoltaic systems. By employing both voltage and d-q axis controllers, the STATCOM demonstrated efficient performance. A comparative analysis with a battery ESS-based STATCOM highlighted the superiority of the SCESS-based approach. Through the simulation of four scenarios, the study confirmed the SCESS-based STATCOM's capability to enhance voltage stability, outperforming BESS-based alternatives and effectively addressing power quality issues. The integration of power quality conditioners, such as UPQCs, in renewable energy systems has been progressing. However, the complexity of control strategies and real-time processing requirements remains a challenge. Hybrid control methods, such as ANNs and ANFIS, have been proposed to improve the performance of the system. However, the optimal control strategy for various system dynamics and environmental conditions remains elusive. The integration of energy storage devices like super capacitors shows potential, but challenges remain in efficient power compensation during transient disturbances. There is a lack of comprehensive solutions that address multiple power quality challenges across diverse renewable energy sources in microgrid systems. Therefore, more integrated and optimized approaches are needed to balance computational efficiency, stability, and adaptability to varying operating conditions.

Qu et al [26]. Proposed a novel two-layer constant power control scheme for wind farms integrating doubly-fed induction generators (DFIGs) with super capacitor-based energy storage systems (ESS) to address wind power intermittency and maintain stable power output to the grid. In their hierarchical control approach, a high-layer Wind Farm Supervisory Controller (WFSC) determines the active power reference for each wind turbine based on grid demand or generation commitments, while the low-layer Wind Turbine Generator (WTG) controllers regulate the individual DFIGs to meet those targets. Deviations between actual wind input and required output are dynamically compensated by the ESS at each turbine, ensuring power smoothing. The proposed scheme was validated through simulation studies on a wind farm comprising 15 DFIG-based turbines in PSCAD/EMTDC, demonstrating the controller's effectiveness in stabilizing active power delivery under variable wind conditions.

Sivasankar et al [27]. Proposed a novel configuration of a Unified Power Quality Conditioner (UPQC) integrated with a super capacitor-based short-term energy storage system to address the challenges of wind power intermittency, especially during grid faults. Unlike conventional compensation devices such as STATCOMs, which address only current-related issues, or Dynamic Voltage Restorers (DVRs), which have limited voltage compensation capabilities, the proposed UPQC system offers enhanced real and reactive power handling and can mitigate voltage sags, negative sequence currents, and power imbalances across a wide operating range (0.1 pu to 0.9 pu). Their model, implemented in MATLAB/SIMULINK, employs a synchronous reference frame-based control strategy for the UPQC, while the energy storage is

Volume 11, Issue 2, December 2025 - ISSN 2356-8569
http://dx.doi.org/10.21622/RESD.2025.11.2.1279

managed via a two-quadrant DC/DC converter. This configuration significantly improves the fault ride-through capability of wind turbine generators and ensures compliance with grid code requirements. Table 2 shows the Comparative analysis of recent advancements in Power Quality Optimization.

Table 2: Comparative analysis of recent advancements in Power Quality Optimization

Author	Techniques Used	Merits	Limitations
Wang et al. [13]	• Finite Control Set Model Predictive Control (FCS-MPC) in dq-frame.	• Simplifies controller structure and reduces complexity compared to traditional linear control methods. • Enhances dynamic power sharing and control using reactive power-based angle estimation.	• Requires accurate system modeling and parameter tuning. • Computationally intensive for real-time applications. • Complex implementation of dynamic power angle estimation.
Das [14]	• Adaptive Neuro-Fuzzy Inference System (ANFIS).	• Effective mitigation of power quality issues like harmonic distortion, voltage sag, and swell. • The hybrid ANFIS-ANN technique achieved the lowest THD.	• Increased complexity in designing and implementing hybrid AI-based control systems. • Performance depends on the quality and volume of training data, especially for ANN and ANFIS.
Lei [15]	• Wind-PV integrated Distributed Generation (DG) system with a Unified Power Quality Conditioner (UPQC).	• · Enables smooth transition between grid-connected and islanded modes without voltage fluctuation. • ·Improves power quality (PQ) by mitigating voltage sag/swell, harmonics, and enhancing power factor (PF).	• Complex control coordination is required between wind, PV, and UPQC for stable operation. • High sensitivity to sudden changes in solar irradiance or wind speed may require advanced predictive control.
Dheeban [16]	• Adaptive Neuro-Fuzzy Inference System (ANFIS).	• Improves power quality. • Enhances fault ride-through capability, provides robust dynamic performance.	• Conventional PI controllers are inadequate during transients and require replacement with advanced controllers. • Complexity in control design increases.
Srilakshmi [17]	• Enhanced Most Valuable Player Algorithm (EMVPA).	• Effective mitigation of PQ issues, such as voltage distortion and THD. • Improved reliability and efficiency in power distribution.	• High complexity in system coordination. • Dependency on accurate modeling and tuning.
Pushkarna [18]	• Unified Power Quality Conditioner (UPQC) applied as a Custom Power Device (CUPS) to mitigate voltage fluctuations in weak grid-connected wind farms.	• Improves power quality and voltage stability at the Point of Common Coupling. • Enhances the compensation capability of UPQC.	• Enhances the compensation capability of UPQC. • Performance heavily depends on accurate design and implementation.
Jin [19]	• Interline AC-DC Unified Power Quality Conditioner (UPQC).	• Enhances Low Voltage Ride Through (LVRT). • Maintains stable DC bus voltage and smooths output power.	• High cost and complexity associated with implementing and maintaining SMES. • Superconducting systems require cryogenic cooling.
Mahar [20]	• Artificial Neural Network (ANN)-based controller for UPQC. • Levenberg-Marquardt backpropagation training.	• Reduces cost and system complexity. • Improves power quality performance. • Lower THD values in load voltage and supply current.	• The training dependency of an ANN can lead to performance degradation if exposed to unseen or noisy data patterns. • Limited interpretability and tuning.

http://dx.doi.org/10.21622/RESD.2025.11.2.1279

Sivakumar [21]	• Enhanced control strategy combining Artificial Neural Network (ANN) and Gravitational Search Algorithm (GSA).	• Improved compensation for PQ issues. • Effective regulation of DC-link voltage.	• Increased computational complexity due to combining ANN and GSA algorithms. • Performance is dependent on the quality of training data.
Yang [22]	• DC Unified Power Quality Conditioner (DC-UPQC) integrated with Dual Active Bridge (DAB).	• Effectively maintains terminal voltage and regulates current in DC-DFIG systems under fault and load variation conditions. • Supports sensitive loads.	• Immaturity of DC custom power protection devices limits current commercial adoption and practical deployment. • Cost and operational challenges due to the requirement for superconducting materials.
Kotla [23]	• Integration of Ultracapacitor (UC) with Unified Power Quality Conditioner (UPQC).	• Improves power quality by mitigating real/reactive power distortions and maintaining voltage stability. • A high-power-density ultracapacitor provides a fast response during transient disturbances.	• Ultracapacitors' low energy density limits their use to short-duration compensation only. • Initial cost and design complexity increase due to additional components like the ultracapacitor and the bidirectional converter.
Döşoğlu [24]	• Decoupled power-based Sliding Mode Control (SMC).	• Enhances dynamic system stability by damping oscillations quickly after disturbances. • Meets grid code compliance while maintaining smooth power output under fault conditions.	• Sliding Mode Control may introduce chattering, which can affect the performance of the power converters. • Implementation complexity increases due to separate modeling and control of stator and rotor EMFs.
Afzal [25]	• Super Capacitor Energy Storage System (SCESS)-based STATCOM.	• · Improves voltage stability, with performance boosting voltage • · Effectively mitigates power quality issues such as voltage drop, harmonic distortion, and reactive power imbalance.	• Lower energy density of supercapacitors limits their ability to provide long-duration backup compared to batteries. • Higher cost per unit of energy stored in supercapacitors can increase system cost for extended applications.
Qu[26]	• High-layer Wind Farm Supervisory Controller.	• The integration of supercapacitor-based ESS at each turbine enables dynamic compensation for wind power fluctuations. • The two-layer control structure (WFSC + WTG controller) allows centralized coordination with decentralized implementation, enhancing scalability and flexibility across large wind farms.	• The study is limited to simulation; real-time performance, especially under hardware and environmental uncertainties, remains untested. • Deploying ESS at each turbine increases system cost and complexity, potentially challenging for large-scale commercial implementation.
Sivasankar [27]	• Unified Power Quality Conditioner (UPQC) integrated with a super capacitor-based short-term energy storage system.	• Enhanced Fault Ride-Through Capability. • Comprehensive Power Quality Compensation.	• High Implementation Complexity and Cost. • Focus Limited to Grid Fault Scenarios.

III. SUPER CAPACITOR-ENHANCED NEURAL CONTROL (SENCO)

Integrating wind energy into microgrids [28] introduces power quality (PQ) issues such as voltage fluctuations, harmonics, and frequency instability, primarily due to the variable and intermittent nature of wind [26]. These challenges necessitate the deployment of compensation devices like passive filters, active filters, and Flexible AC Transmission System (FACTS) controllers to enhance voltage stability and reduce total harmonic distortion (THD).

http://dx.doi.org/10.21622/RESD.2025.11.2.1279

Among these, the Unified Power Quality Conditioner (UPQC) serves as a comprehensive solution that combines both series and shunt active power filters. This configuration effectively mitigates voltage and current disturbances, compensates reactive power, and suppresses harmonics. To further improve the dynamic performance of UPQCs, advanced control techniques such as Artificial Neural Networks (ANN) are integrated to generate optimized Pulse Width Modulation (PWM) signals, enabling faster and more adaptive responses compared to conventional Proportional-Integral-Derivative (PID) controllers. To address persistent limitations such as slow response and limited compensation accuracy, this work proposes a novel SENCO (Stabilizing Energy through Neural-Controlled Optimization) approach, illustrated in Figure 1. This method incorporates ultra-capacitors into the UPQC framework, providing short-term energy storage to buffer transient power fluctuations from wind turbines during grid disturbances or disconnections. By employing adaptive control and iterative parameter tuning, the proposed ANN-based strategy enhances the stability and power quality of wind-integrated microgrids, making the UPQC a robust solution for renewable-based distributed energy systems.

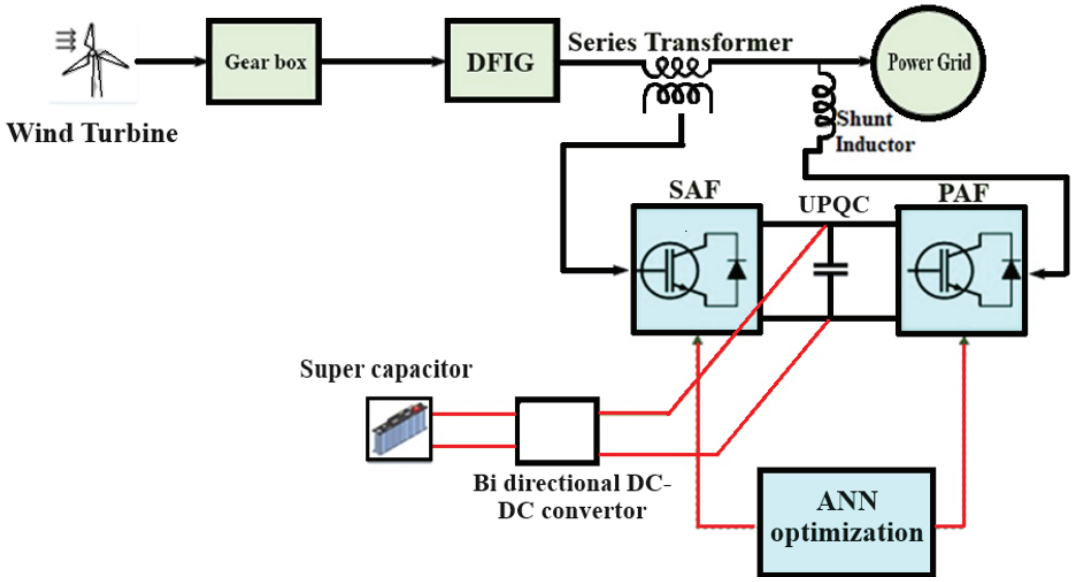

Figure 1: Architecture of Super Capacitor-Enhanced Neural Control System.

A. Modelling of a Wind turbine

Wind turbines are energy conversion systems designed to harness kinetic energy from wind and transform it into mechanical energy, which is then converted into electrical energy using a generator. When integrated into a microgrid, they optimize energy generation and maintain power quality. The turbine generates AC electricity, which is transmitted to the microgrid via a power converter. The microgrid consists of an Energy Storage System, which stores excess energy during high wind conditions and releases it during low wind periods. There are various types of wind turbines, among which two-axis turbines are frequently used. In our research, we utilize these two different turbine types to analyze the effectiveness of the proposed SENCO system. Wind turbines serve as critical renewable energy sources, requiring advanced control mechanisms like UPQCs to maintain power quality by using a shunt converter and a series converter to address voltage issues, harmonic distortion, and power intermittency. These systems ensure stable and efficient energy delivery by compensating for wind power variability and enhancing the overall power quality through adaptive algorithms, such as ANN-based PWM control, and energy storage solutions like supercapacitors. The UPQC monitors and adjusts power flow, using stored energy from the supercapacitors to ensure an uninterrupted supply. The system maintains grid stability through real-time feedback.

1. DFIG

A wind turbine equipped with a DFIG uses a back-to-back voltage source converter to supply power to the rotor winding. This rotor is connected to the grid through a gearbox, as illustrated in Figure 2 [27].

http://dx.doi.org/10.21622/RESD.2025.11.2.1279

The stator winding of DFIG is connected to the grid, while the rotor winding is linked to the rotor-side converter (RSC), and the grid-side converter (GSC) feeds the rotor winding. A DC-link is incorporated to decouple the electrical grid frequency from mechanical rotor frequency, allowing for variable-speed operation. However, the converter's limited capacity restricts its voltage control capability when compared to a synchronous generator. The back-to-back converter features current control loops, which enhance the controllability of the turbine. Grid-side converter operates at a unity power factor, preventing overloading during high wind speeds. To limit the speed of the rotor, blades are pitched, which reduces the mechanical power extracted from the wind and restores the balance between mechanical and electrical power, preventing the speed of the rotor from exceeding safe limits.

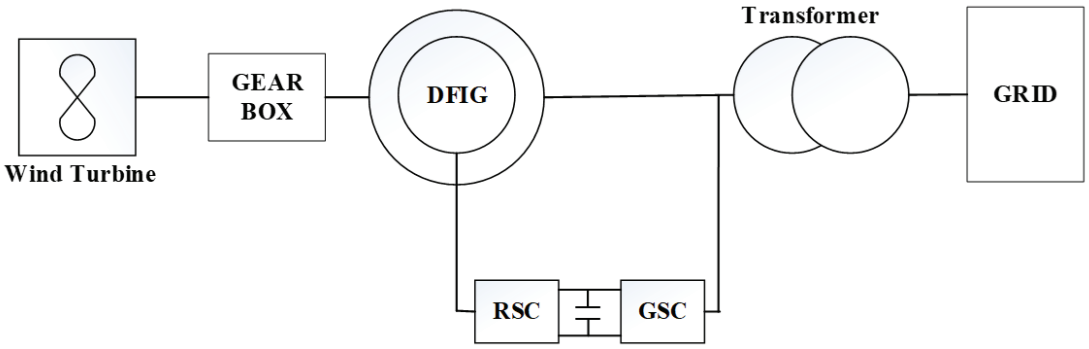

Figure 2: Configuration of a DFIG wind turbine connected to a grid.

The power of the rotor side is given as [29]

$$P_r = v_{dr} i_{dr} + v_{qr} i_{qr} \quad (1)$$

$$Q_r = v_{qr} i_{dr} - v_{dr} i_{qr} \quad (2)$$

Power at the stator side is given by

$$P_s = v_{ds} i_{ds} + v_{qs} i_{qs} \quad (3)$$

$$Q_s = v_{qs} i_{ds} - v_{ds} i_{qs} \quad (4)$$

Total output power is

$$P = P_s + P_r = v_{dr} i_{dr} + v_{qr} i_{qr} + v_{ds} i_{ds} + v_{qs} i_{qs} \quad (5)$$

$$Q = Q_s + Q_r = v_{qs} i_{ds} + v_{qr} i_{dr} - v_{ds} i_{qs} - v_{dr} i_{qr} \quad (6)$$

B. Proposed Unified Power Quality Conditioner

The UPQC employs both shunt and series active filters that are interconnected through a shared DC link and capacitor [30]. The shunt component addresses load-side issues such as harmonic currents, low power factor, and load imbalance by injecting compensating currents that are sinusoidal and in phase with the source voltage. In contrast, the series component mitigates supply-side disturbances, including voltage sags, flickers, unbalance, and harmonics, by injecting voltage through the line. The UPQC system comprises several essential components: the AC supply, which represents the utility grid; the injection transformer, responsible for injecting compensating voltage into the supply line; the series converter, a voltage source converter connected in series to address voltage-related issues; and the shunt converter, which provides current compensation to eliminate harmonics, reactive power, and load imbalance. The DC link capacitor connects both converters, allowing power exchange while also functioning as an energy storage element to maintain a stable DC voltage. The UPQC controller generates reference signals for both converters, calculates compensating currents and voltages based on detected disturbances, and ensures their coordinated operation. The load refers to the electrical system or equipment supplied by the UPQC, which may exhibit nonlinear characteristics or sensitivity to voltage fluctuations. In wind turbine-integrated microgrid systems, issues such as voltage disturbances, harmonic currents, and power imbalances are common. The UPQC provides an effective and flexible solution to these power quality challenges by utilizing its integrated series and shunt compensation capabilities.

1. Voltage and Current Control

In the research, the Park transformation (dq0) is used, a widely adopted mathematical approach, to control voltage. This transformation decouples variables, simplifies time-varying equations,

http://dx.doi.org/10.21622/RESD.2025.11.2.1279

and refers variables to a shared reference frame. This method is applicable to any three-phase, time-varying signal, regardless of whether it is sinusoidal or distorted. In steady-state conditions, the fundamental component of the waveform is converted into a constant DC term, which represents the key benefit of the $dq0$ transformation. A synchronous reference frame control strategy, based on $dq0$ transformation, is implemented to manage series and shunt converters concurrently. In shunt compensation, a synchronous $dq0$ reference frame is constructed using the system's actual current. In this approach, the positive-sequence component is aligned with the d-axis, while the negative and zero-sequence components are aligned with the q and zero axes of the system current, respectively. The following expressions are given as

$$\begin{bmatrix} I_d \\ I_q \\ I_o \end{bmatrix} = \sqrt{\frac{2}{3}} \begin{bmatrix} \cos\theta_d & cos\,(\,\theta_d\, -\, 2\pi/3\,) & cos\,(\,\theta_d\, +\, 2\pi/3\,) \\ -sin\,\theta_d & -\,sin\,(\,\theta_d\, -\, 2\pi/3\,) & -\,sin\,(\theta_d\, +\, 2\pi/3\,) \\ 1\,/\sqrt{2} & 1\,/\sqrt{2} & 1\,/\sqrt{2} \end{bmatrix} \begin{bmatrix} I_a \\ I_b \\ I_c \end{bmatrix} \tag{7}$$

Above equation $\theta_d = \omega_d + \varphi$, where ω_d is the angular velocity of the signals and φ is the initial angle.

$$\begin{bmatrix} I_d \\ I_q \\ I_o \end{bmatrix} = \sqrt{\frac{3}{2}} \left\{ \begin{bmatrix} I_{p\cos\theta_p} & I_{n\cos(2\omega t+\theta_n} \\ I_{p\sin\theta_p} & +\,-I_{n\sin(2\omega t+\theta_n} \\ 0 & 0 \end{bmatrix} \right\} \tag{8}$$

The anticipated compensation current necessary for voltage recovery is determined by assigning the d-coordinate current to the rated peak current. Reactive power compensation is achieved by nullifying the components.

$$\begin{bmatrix} I_d \\ I_q \\ I_o \end{bmatrix} = \begin{bmatrix} I_{p\cos\theta_p} \\ 0 \\ 0 \end{bmatrix} \tag{9}$$

The reference current is determined by combining the active current loss with the average current component, as illustrated below.

$$I_d' = I_d + I_{dloss} \tag{10}$$

The $dq0$ reference current obtained is subsequently converted into abc reference components.

$$\begin{bmatrix} I_a{}' \\ I_b{}' \\ I_c{}' \end{bmatrix} = \sqrt{\frac{2}{3}} \begin{bmatrix} \cos\theta_d & -sin\,\theta_d & 1\,/\sqrt{2} \\ cos\,(\,\theta_d\, -\, 2\pi/3\,) & -\,sin\,(\,\theta_d\, -\, 2\pi/3\,) & 1\,/\sqrt{2} \\ cos\,(\,\theta_d\, +\, 2\pi/3\,) & -\,sin\,(\,\theta_d\, +\, 2\pi/3\,) & 1\,/\sqrt{2} \end{bmatrix} \begin{bmatrix} I_d{}' \\ 0 \\ 0 \end{bmatrix} \tag{11}$$

The reference currents are compared with actual system currents measured using a hysteresis current controller to generate converter switching signals. This shunt compensation effectively addresses current-related issues. For series compensation, voltage is converted into *the* $dq0$ axis using the Park transformation, which results in the following equation.

$$\begin{bmatrix} I_d \\ I_q \\ I_o \end{bmatrix} = \sqrt{\frac{2}{3}} \begin{bmatrix} \cos\theta_d & cos\,(\,\theta_d\, -\, 2\pi/3\,) & cos\,(\,\theta_d\, +\, 2\pi/3\,) \\ -sin\,\theta_d & -\,sin\,(\,\theta_d\, -\, 2\pi/3\,) & -\,sin\,(\theta_d\, +\, 2\pi/3\,) \\ 1\,/\sqrt{2} & 1\,/\sqrt{2} & 1\,/\sqrt{2} \end{bmatrix} \begin{bmatrix} v_a \\ v_b \\ v_c \end{bmatrix}$$

$$= \sqrt{\frac{3}{2}} \left\{ \left[\begin{bmatrix} v_{p\cos\emptyset_p} \\ v_{p\sin\emptyset_p} \\ 0 \end{bmatrix} + \begin{bmatrix} v_{n\cos(2\omega t+\emptyset_n} \\ -v_{n\sin(2\omega t+\emptyset_n} \\ 0 \end{bmatrix} + \begin{bmatrix} 0 \\ 0 \\ v_{0\cos(2\omega t+\emptyset_0} \end{bmatrix} \right] \right\} = \begin{bmatrix} v_{dp} \\ v_{qp} \\ 0 \end{bmatrix} + \begin{bmatrix} v_{dn} \\ v_{qn} \\ 0 \end{bmatrix} + \begin{bmatrix} 0 \\ 0 \\ v_{00} \end{bmatrix} \tag{12}$$

Here $\emptyset_{,p}$ - difference in phase between positive-sequence component and reference voltage. Hence, with a minimal phase difference, U_d provides an estimation of input voltage amplitude while U_q convey information regarding phase error. Figure 3 shows the synchronous reference frame control strategies.

http://dx.doi.org/10.21622/RESD.2025.11.2.1279

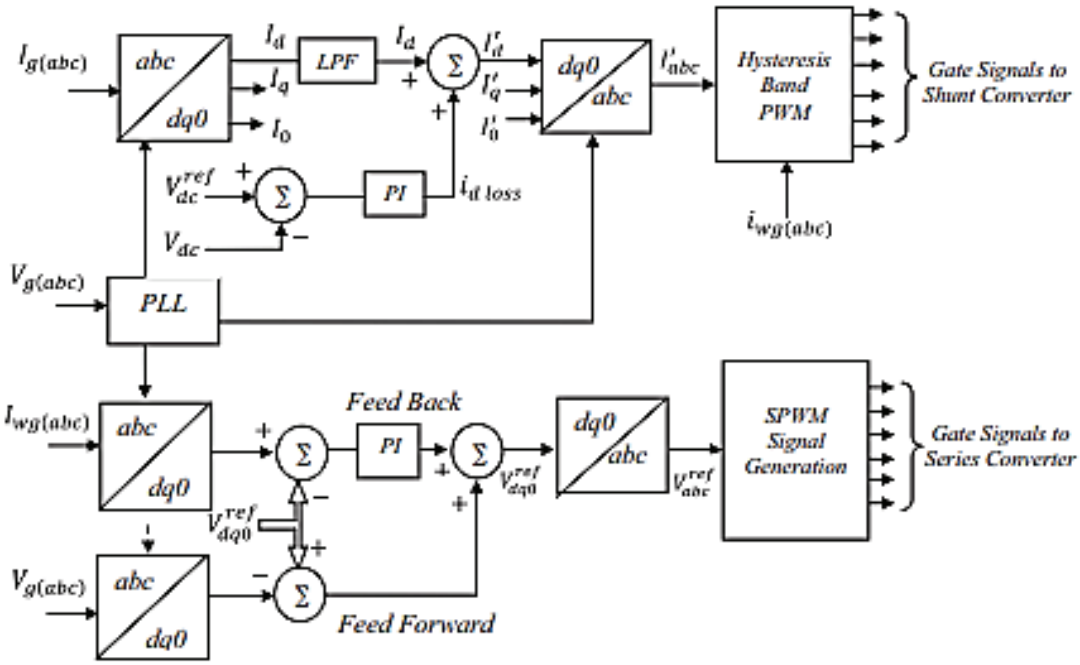

Figure 3: Synchronous reference frame control strategies.

According to the above equation, the components at DC are derived from the positive sequence of *the dq0* reference frame. Hence, the v_{dp} of the above equation is maintained as while v_M all other components are effectively removed through compensation voltage. The reference voltage is given by

$$\begin{bmatrix} v_d \\ v_q \\ v_0 \end{bmatrix} = \begin{bmatrix} v_m \\ 0 \\ 0 \end{bmatrix} \quad (13)$$

The injection voltage control involves grid voltage feedforward and wind generator voltage feedback. A PI regulator is used to equalize the difference between voltage and injected voltage in series with line due to inverter's output filter. The regulator output is added to DVR, improving system response speed and calculating the required modulation depth to inject the difference between grid and reference voltages.

$$v'_d = v_d + \Delta v \quad (14)$$

The u'_d reference voltage is then subsequently transformed into the abc reference frame.

$$\begin{bmatrix} v_a \\ v_b \\ v_c \end{bmatrix} = \sqrt{\frac{2}{3}} \begin{bmatrix} \cos\theta_d & -\sin\theta_d & 1/\sqrt{2} \\ \cos(\theta_d - 2\pi/3) & -\sin(\theta_d - 2\pi/3) & 1/\sqrt{2} \\ \cos(\theta_d + 2\pi/3) & -\sin(\theta_d + 2\pi/3) & 1/\sqrt{2} \end{bmatrix} \begin{bmatrix} v_d' \\ 0 \\ 0 \end{bmatrix} \quad (15)$$

These reference voltage values are then compared with the actual measured voltage at the Point of Common Coupling. Based on this comparison, the switching signals for the series converter are generated using the SPWM technique.

2. ESS configuration and control

Super capacitors are integrated into UPQC systems to handle short-term power disturbances, such as voltage sags, swells, and rapid fluctuations in power generation, especially from renewable sources like wind turbines. They serve as high-speed energy storage solutions, providing rapid compensation for energy imbalances between series and shunt converters. Energy storage devices are used for short-term energy buffering, which helps control power variations brought on by variations in wind speed, especially when there is a power drop or low wind. This is often accomplished via super capacitors and batteries, which store surplus energy during periods of high wind speeds and release it during periods of low wind speeds. These devices lessen the need

http://dx.doi.org/10.21622/RESD.2025.11.2.1279

for costly backup generators, regulate power output, and guarantee a steady supply. Energy stored in a capacitor can be described by

$$E = ½ CV^2 \quad (16)$$

Here E denotes the stored energy in J, C is the capacitance of the super capacitor in farad, and V is the voltage across the capacitor in volts. This energy can be discharged back to system when required to offset a drop in wind power generation.

The power transmitted between ESS and the grid can be expressed as

$$P_{storage} = C\frac{dv}{dt} \quad (17)$$

$P_{storage}$ is power exchanged by the system in watts and $\frac{dv}{dt}$ is rate of change of voltage across the storage system in volts per second. The storage system releases stored energy when wind power decreases rapidly, and stores excess energy during high generation periods.

The DC link capacitor stores and exchanges energy between converters, supplying or absorbing power to maintain system stability during voltage or current disturbances.

$$P_{series} + P_{shunt} = P_{DC-link} + P_{supercapacitor} \quad (18)$$

Here $P_{supercapacitor}$ is the power supplied or absorbed by the supercapacitor. The UPQC system uses energy exchange and storage to stabilize power flow, reduce voltage fluctuations, and maintain power quality during transients [31]. An Energy Storage System (ESS), especially using super capacitors, acts as a buffer to handle power variability in wind energy systems. Super capacitors are ideal due to their fast charge/discharge capability and high capacitance. Integrated control systems manage their operation to optimize performance and lifespan. This helps mitigate wind intermittency, ensuring stable and reliable power delivery.

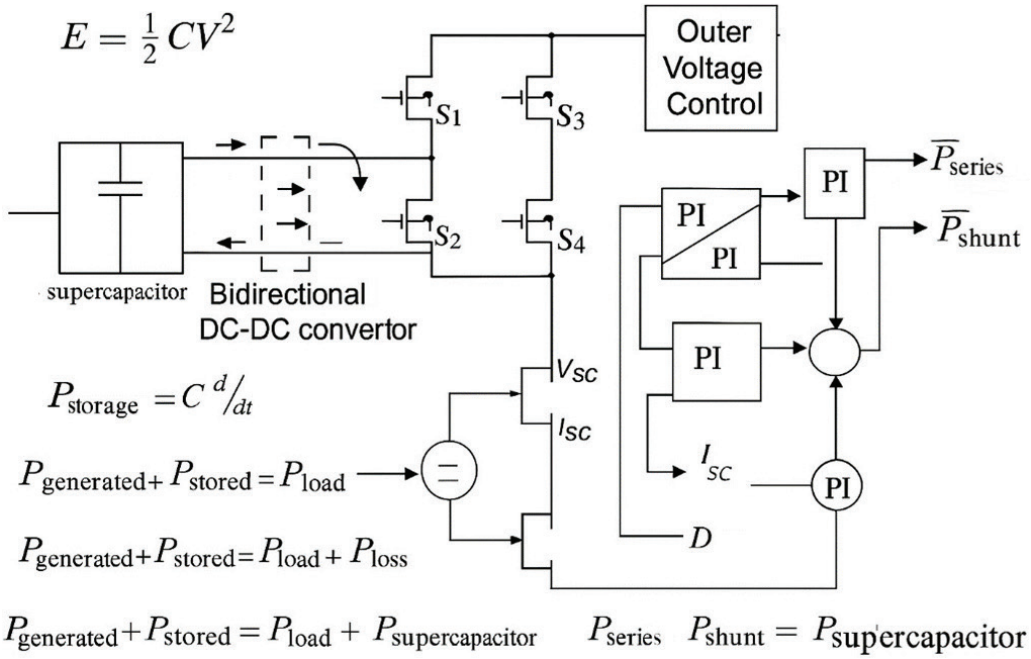

Figure 4: ESS control Methodology.

The schematic diagram in Figure 4 illustrates the control methodology for integrating a supercapacitor-based Energy Storage System (ESS) into a UPQC architecture using a bidirectional DC-DC converter. The outer voltage control loop maintains the supercapacitor voltage V_{SC}, while the inner current loop controls the charging/discharging current I_{SC} via a duty cycle D for the converter switches S_1 - S_4. PI controllers regulate both current and voltage to ensure stable power exchange. The stored energy is defined by $E\,\frac{1}{2}mv^2$, and the power exchange with the grid is governed by $P_{Storage} = C\frac{dV}{dt}$. The energy balance is maintained across the system using equations $P_{generated} + P_{Storage} = P_{Load} + P_{Loss}$, and during transients, the supercapacitor compensates for power imbalances, supporting both series and shunt branches of the UPQC.

Volume 11, Issue 2, December 2025 - ISSN 2356-8569
http://dx.doi.org/10.21622/RESD.2025.11.2.1279

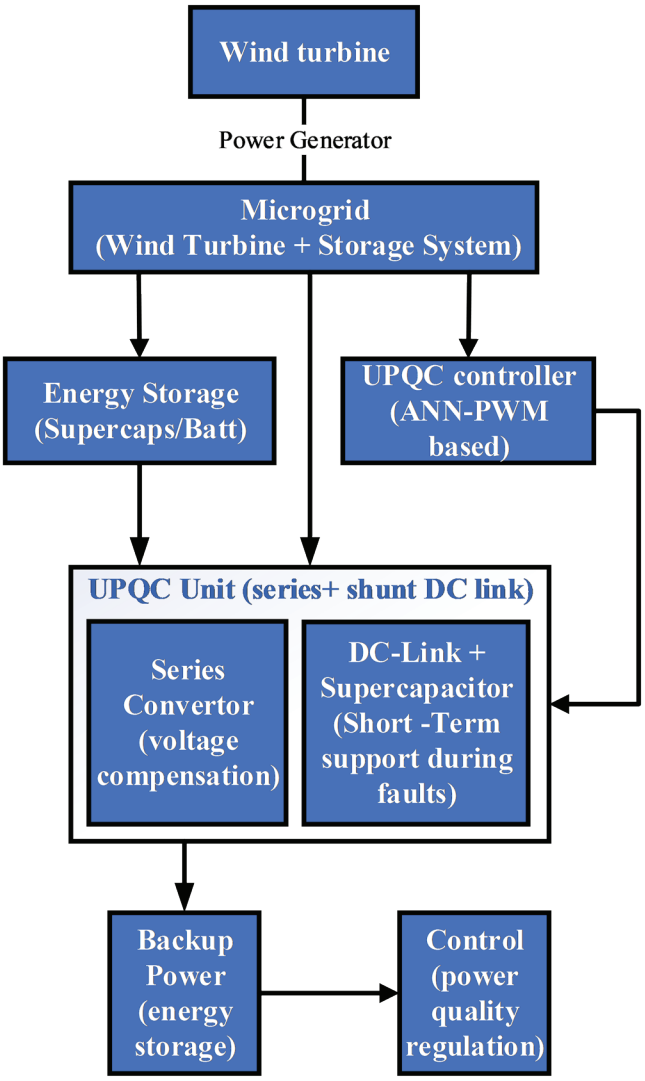

Figure 5: Integration of short-term energy buffering and microgrid disconnection.

The flowchart in Figure 5 illustrates a power quality enhancement framework in a wind energy-based microgrid using a UPQC with an Artificial Neural Network-based PWM controller. The system begins with a wind turbine connected to a power generator, forming the primary source in the micro grid, which also includes energy storage units such as super capacitors or batteries. This setup is managed by a UPQC controller, which employs an ANN-PWM-based algorithm to optimize switching and regulation. The energy from the generator and storage flows into the UPQC unit, comprising a series converter (for voltage compensation) and a DC-link integrated with super capacitors to provide short-term fault ride-through support. The UPQC thus ensures both voltage and current compensation. The system provides backup power via energy storage and includes a control block for overall power quality regulation, making it robust against disturbances and enhancing reliability in renewable-based micro grids.

The microgrid must maintain a balance between power generation, storage, and consumption during an islanding event, as mathematically expressed.

$$P_{generated} + P_{stored} = P_{load} + P_{loss} \quad (19)$$

Where $P_{generated}$ is power generated by the turbine, P_{stored} is power drawn from the ESS, P_{load} denotes the power consumed by the loads in the microgrids, and P_{loss} is the power losses in the system. The ESS needs to supply P_{stored} to balance the generation and load. If there is an excess of wind power, the system stores the surplus in the super capacitor for later use.

3. Adaptive PWM Control Algorithm based on ANN

In contemporary microgrid systems, the UPQC plays a vital role in mitigating power quality disturbances such as voltage sags, harmonic distortions, and current imbalances. Its core function involves dynamic adjustment of PWM signals in voltage source converters, based on real-time monitoring of system parameters. These dynamic adjustments ensure stable voltage and current delivery to sensitive loads. To enhance the responsiveness of the UPQC, adaptive control strategies, particularly those based on ANNs, are employed. Unlike conventional controllers with fixed parameters, ANN-based control algorithms analyse input parameters such as voltage deviations, harmonic distortion levels, and load conditions to generate optimal PWM signals. These signals drive the UPQC's series and shunt converters to maintain voltage stability, reduce THD, and improve power factor. ANN-based PWM optimization is especially beneficial in renewable energy-integrated micro grids, where the system must adapt to intermittent generation and fluctuating load demands [32]. By learning from historical system data and making predictive, real-time adjustments, ANN controllers improve the system's fault ride-through capability and overall reliability. A detailed control block diagram of the proposed ANN-based PWM Control Structure for UPQC is shown in Figure 6, illustrating the interaction between the ANN, PWM generator, UPQC control, and feedback mechanisms [33].

http://dx.doi.org/10.21622/RESD.2025.11.2.1279

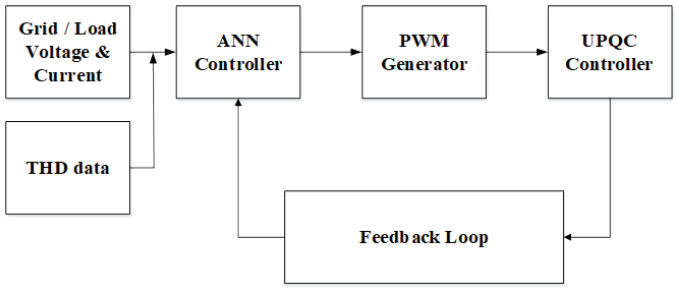

Figure 6: ANN-Based Adaptive PWM Control Structure for UPQC.

3.1. ANN Architecture

The ANN structure used in the proposed SENCO model is a three-layer feedforward neural network consisting of three layers, and Table 3 shows the training parameters.

- Input Layer (3 neurons):

$$x_1 = V_{\text{grid}}, x_2 = I_{\text{load}}, x_3 = V_{DC-\text{link}} \quad (20)$$

- Hidden Layer (5 neurons) with sigmoid activation:

$$h_j = f\left(\sum_{i=1}^{3} w_{ij}^{(1)} x_i + b_j^{(1)}\right), f(x) = \frac{1}{1+e^{-x}} \quad (21)$$

- Output Layer (2 neurons): PWM reference values for series and shunt converters

$$y_k = \sum_{j=1}^{5} w_{jk}^{(2)} h_j + b_k^{(2)} \quad (22)$$

Table 3: Training parameters

Features	Parameters
Algorithm	Levenberg-Marquardt backpropagation
Loss Function	Mean Squared Error (MSE)
Learning Rate	0.01

3.2. Design Procedure

The design of the adaptive ANN-based control scheme begins with the collection of time-series data for voltage and current under both faulted and normal grid conditions. These data points serve as the training dataset for the neural network. To ensure uniformity and enhance learning convergence, all input parameters are normalized within the range of -1 to 1. The network is then trained offline using a supervised learning approach, where the target PWM signals are derived from an optimal control model. During training, the ANN adjusts its internal parameters to minimize the error between the predicted and target PWM outputs using the Levenberg-Marquardt backpropagation algorithm. After satisfactory performance is achieved in offline training, the trained ANN is integrated into the UPQC controller block in Simulink, enabling real-time operation. In the online stage, the ANN dynamically receives real-time grid voltage, load current, and DC-link voltage as inputs and produces optimal PWM control signals for both series and shunt converters of the UPQC. To improve the learning efficiency, initial Weights $w_{ij}^{(1)}, w_{jk}^{(2)}$ are initialized using Xavier initialization

$$w \sim \mathcal{U}\left(-\sqrt{\frac{6}{n_{\text{in}}+n_{\text{out}}}}, \sqrt{\frac{6}{n_{\text{in}}+n_{\text{out}}}}\right) \quad (23)$$

Where n_{in} and n_{out} are the number of neurons in the previous and the subsequent layers, respectively, this initialization technique helps prevent vanishing or exploding gradients during training and improves convergence.

The combination of ANN-based intelligence and adaptive control techniques offers significant performance benefits. The ANN enables the UPQC to autonomously adapt to varying load or grid conditions, while adaptive control ensures system stability and convergence even under dynamic disturbances. Together, they allow the UPQC to deliver fast, precise, and stable compensation, enhancing both power quality and system efficiency. This integrated control approach makes the UPQC a powerful solution for ensuring reliable and high-quality power delivery in modern microgrid and renewable energy-based systems.

IV. Result and discussion

The results and discussion highlight the challenges of integrating wind energy into microgrids, particularly in maintaining power quality, which are effectively mitigated using FACTS devices like UPQC.

A. Implementation setup

The implementation setup of the proposed model is given below. The detailed electrical and control system specifications used for simulating the proposed SENCO-based UPQC model are provided in Table 4.

Volume 11, Issue 2, December 2025 - ISSN 2356-8569
http://dx.doi.org/10.21622/RESD.2025.11.2.1279

Table 4: Electrical and Control System Parameters Used in the Proposed SENCO Model

Component	Parameter	Value	Unit
Wind Turbine (DFIG)	Rated Power	2.0	MW
	Rated Voltage	690	V (rms, line-ground)
	Rated Frequency	50	Hz
	Rated Speed	1500	rpm
Grid	Voltage	400	V (rms)
	Frequency	50	Hz
	Short Circuit Capacity	10	MVA
Converters (VSC)	Rated Power	2.2	MVA
	DC-Link Voltage	700	V
	Switching Frequency	10	kHz
DC Link	Capacitance	4700	μF
	Rated Voltage	700	V
Supercapacitor Bank	Capacitance	50	F
	Rated Voltage	200	V
	Max Energy Stored	1000	kJ
Control Parameters	ANN Hidden Layers	2	—
	ANN Learning Rate	0.01	—
	PI Controller Kp / Ki (shunt & series paths)	0.8 / 0.05	—

These include wind turbine generator ratings, converter and grid parameters, supercapacitor storage configuration, and key controller settings. These values ensure a realistic simulation of grid-connected wind systems and validate the UPQC's performance under dynamic conditions.

B. *Input parameters*

The graph in Figure 7 shows the dynamic behavior of a wind energy system over time, illustrating fluctuations in active power, reactive power, wind voltage, and wind current.

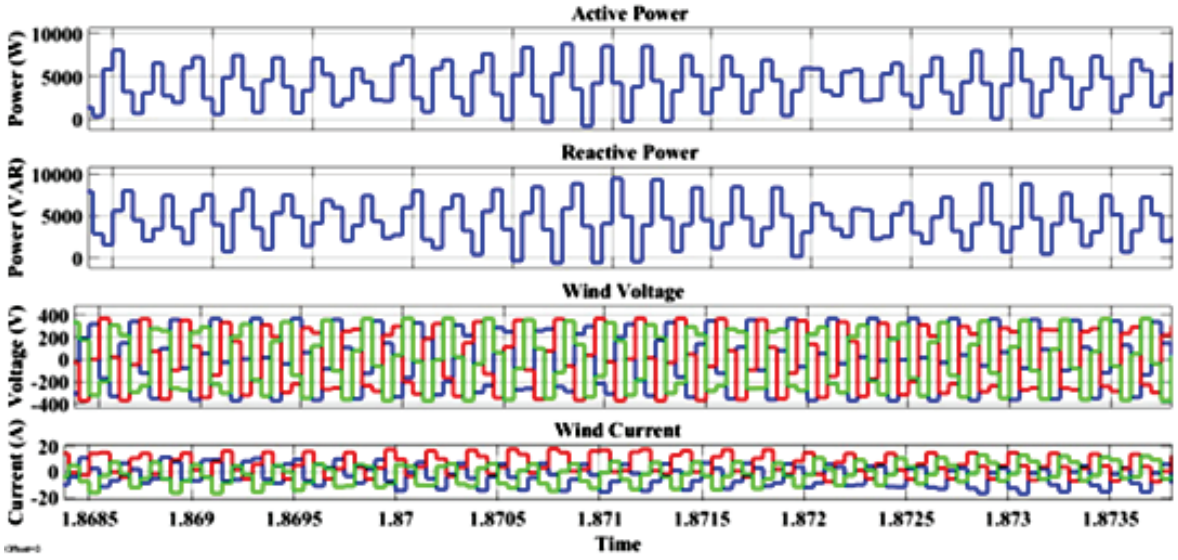

Figure 7: Rotor active power of DFIG with UPQC for the proposed model.

Volume 11, Issue 2, December 2025 - ISSN 2356-8569
http://dx.doi.org/10.21622/RESD.2025.11.2.1279

The active power graph reveals significant fluctuations between negative and positive values, with sharp peaks reaching up to 15 kW and dips below -5 kW. These variations are characteristics of wind turbines, which experience the intermittent nature of wind. Such fluctuations can also result from sudden changes in wind speed or disturbances in the grid. The reactive power graph, with values up to 10^5 VAR, shows smaller, less pronounced fluctuations, indicating the system's ability to withstand voltage disturbances, ensuring stability in power factor and voltage regulation. The wind voltage graph fluctuates between -400 V and 400 V, showing significant instability with sharp voltage spikes and dips, which could be indicative of voltage sags, swells, or harmonics in the system. These fluctuations can be caused by grid faults or rapid changes in turbine load. Similarly, the wind current graph displays current variations between -2000 A and 2000 A, reflecting variable power output and dynamic load conditions in wind turbines. The sharp changes in current may result from rapid transitions in power generation or reactive power compensation. Collectively, the graphs show that the system experiences substantial power quality issues, such as voltage instability and harmonic distortions, which are common in renewable energy systems like wind power. These issues underscore the need for power conditioning devices such as UPQC and FACTS devices, which are essential for mitigating disturbances and stabilizing the grid. The significant fluctuations in active and reactive power, voltage, and current highlight the importance of implementing effective control mechanisms to ensure stable power quality in microgrids, especially those integrating variable renewable energy sources like wind turbines.

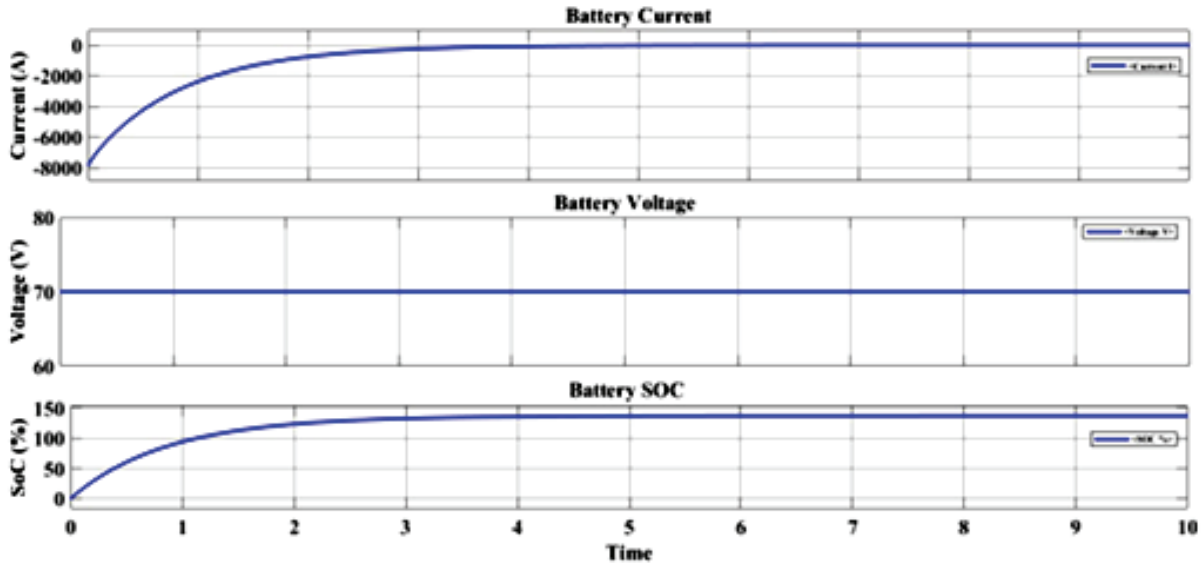

Figure 8: Battery output of DFIG with UPQC for the proposed model.

The graph provided in Figure 8 consists of three plots illustrating the performance of a battery system over a 10-second interval, focusing on battery current, voltage, and SoC. The battery current starts at 0 A and gradually decreases, reaching approximately -8000 A by the end of the simulation. This indicates a high rate of current draw, likely during a charging or discharging process. The battery voltage remains constant at around 70 V throughout the simulation, showing stable voltage regulation despite changes in current. The SoC starts at 0% and steadily increases, reaching approximately 100% by the end of the 10 seconds. This suggests a consistent charging process where the battery reaches full capacity within the observed time frame. The stability in voltage and the controlled increase in SoC reflect the efficiency of the battery management system in regulating charging operations.

http://dx.doi.org/10.21622/RESD.2025.11.2.1279

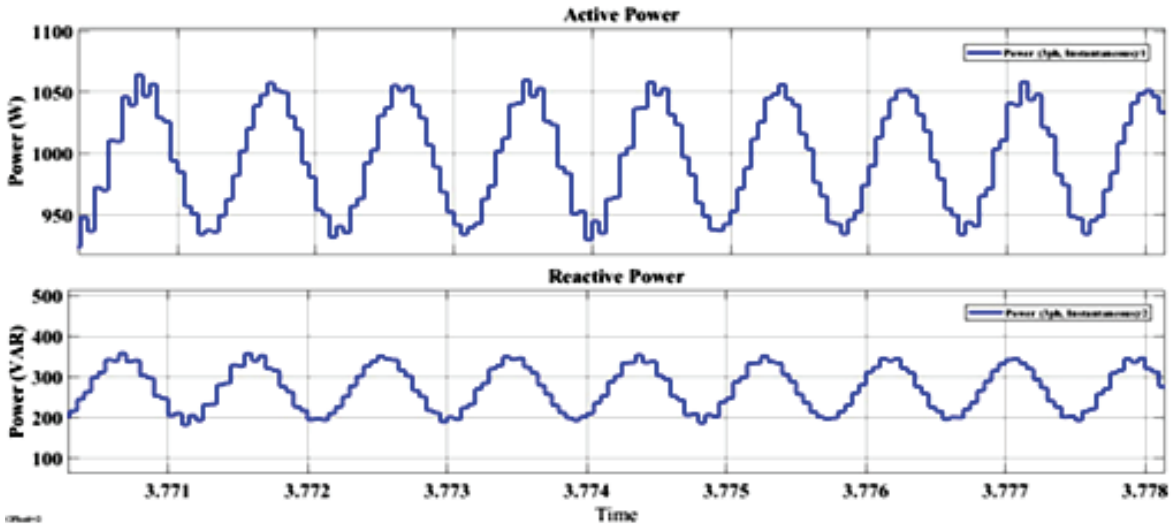

Figure 9: Grid output of DFIG with UPQC for the proposed model.

The graph in Figure 9 consists of two plots: active and reactive powers over time. In the active power graph, the power stabilizes near 999 W, with minimal oscillations observed between 999 W and 999.8 W. This stability indicates effective power delivery by the system, suggesting minimal impact from disturbances or wind fluctuations. The reactive power graph shows a constant value of approximately 0.01 VAR, remaining close to zero throughout the observed time. This indicates that the system maintains an almost unity power factor with negligible reactive power flow, demonstrating effective voltage regulation and optimal grid operation. Overall, these graphs represent a well-functioning system with stable power output and minimal reactive power demand, likely achieved through efficient control strategies and compensating devices.

C. Dynamic Interaction between UPQC and DFIG Converters

In the proposed SENCO framework, the dynamic interaction between the UPQC and the wind turbine converters DFIG is critically considered. The UPQC, operating with ANN-based adaptive PWM control, continuously monitors and responds to voltage and current fluctuations induced by the wind energy conversion systems. In the DFIG configuration, the UPQC supports the grid-side converter in maintaining voltage stability during rotor flux variations and active/reactive power oscillations. Simulation results clearly show that the UPQC significantly dampens voltage and current oscillations from the DFIG generator, ensuring improved power quality and converter stability. These results confirm the coordinated and beneficial interaction between the UPQC and the converter systems, highlighting the effectiveness of the integrated control strategy.

1. Without UPQC

This represents the system operating without any compensation mechanism. The grid is subjected to faults and nonlinear load disturbances. As expected, power quality significantly deteriorates due to the absence of any mitigating device. The voltage and current waveforms show heavy distortion, high THD, and imbalanced phase profiles. This case sets the baseline for comparing improvements from subsequent methods.

http://dx.doi.org/10.21622/RESD.2025.11.2.1279

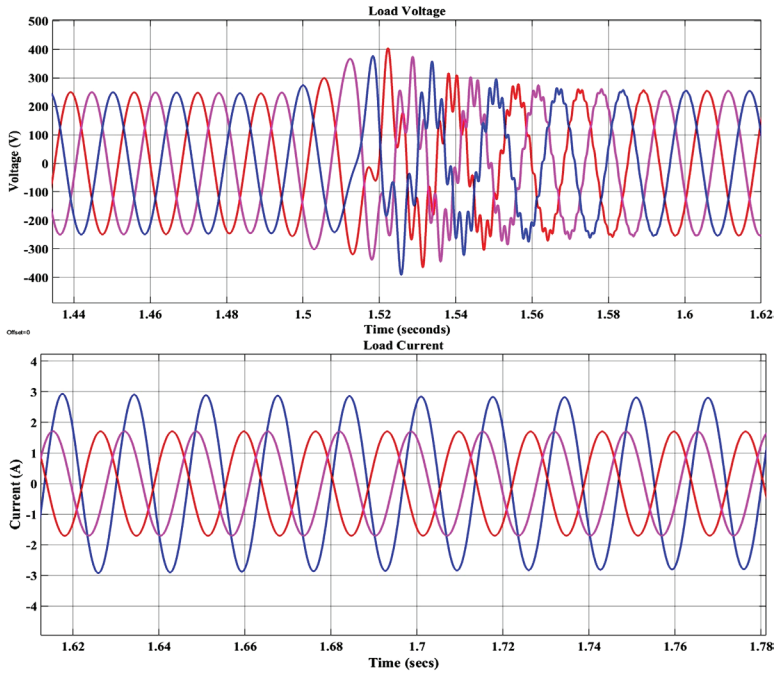

Figure 10: Comparison of voltage and current of DFIG without UPQC.

The graphs in Figure 10 show the behavior of load voltage and load current under different operating conditions. The load voltage waveform experiences disturbances around 1.52 seconds, causing fluctuations and distortions. This was due to an intentionally applied unbalanced nonlinear load, which was designed to create an asymmetrical loading scenario. This allows for better evaluation of UPQC performance under non-ideal grid conditions in subsequent cases. The load current waveform follows a clean sinusoidal shape, initially disrupting current flow around 1.68 seconds. However, it stabilizes shortly afterward, restoring sinusoidal characteristics and maintaining a balanced amplitude between ±4A. The graphs highlight the system's ability to handle disturbances and maintain stable voltage and current waveforms, ensuring reliable power quality and minimal disruptions to connected loads.

2. Case 2: With UPQC

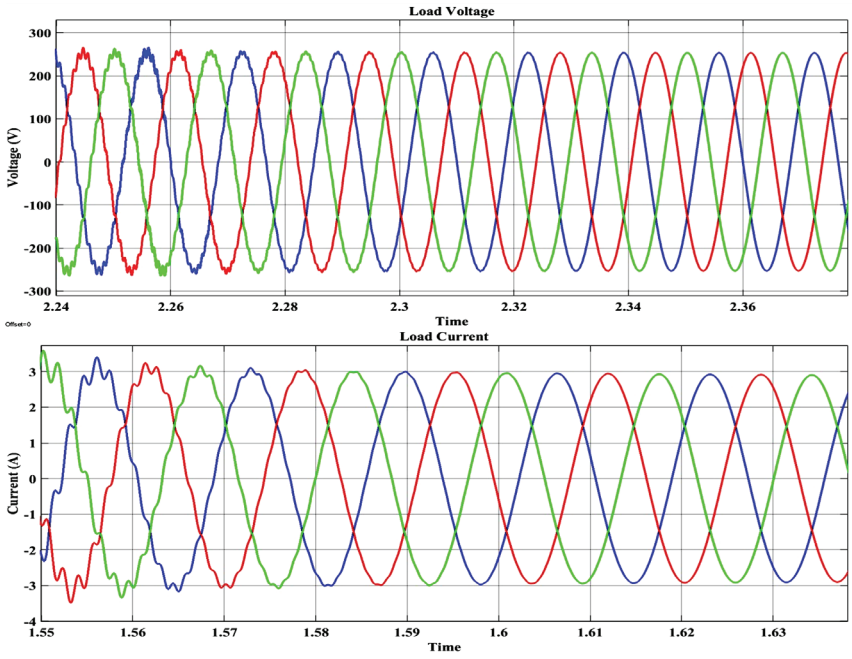

Figure 11: Comparison of voltage and current of DFIG without a capacitor.

Volume 11, Issue 2, December 2025 - ISSN 2356-8569
http://dx.doi.org/10.21622/RESD.2025.11.2.1279

Figure 11 presents the load voltage and load current waveforms in a three-phase system under the operation of an ANN-based UPQC controller. The top plot shows the three-phase load voltage (red, green, and blue) over the time interval of approximately 2.24 to 2.37 seconds. Initially, there are minor distortions in the voltage waveform, but as time progresses, the voltages stabilize into smooth, balanced sinusoidal waveforms with peak amplitudes close to ±300 V, indicating successful voltage compensation by the UPQC. The bottom plot displays the corresponding load current waveforms over the time interval of approximately 1.55 to 1.635 seconds. At the beginning of this interval, the currents are clearly distorted and unbalanced, with visible harmonic content and asymmetry among the phases. However, after about 1.58 seconds, the current waveforms become balanced, sinusoidal, and symmetrical, each reaching a peak amplitude of around ±3.5 A. This transition demonstrates the effective mitigation of harmonic distortion and imbalance by the UPQC system. Overall, the figure confirms that the ANN-controlled UPQC successfully restores both voltage and current waveforms to high-quality sinusoidal conditions, ensuring improved power quality at the load side.

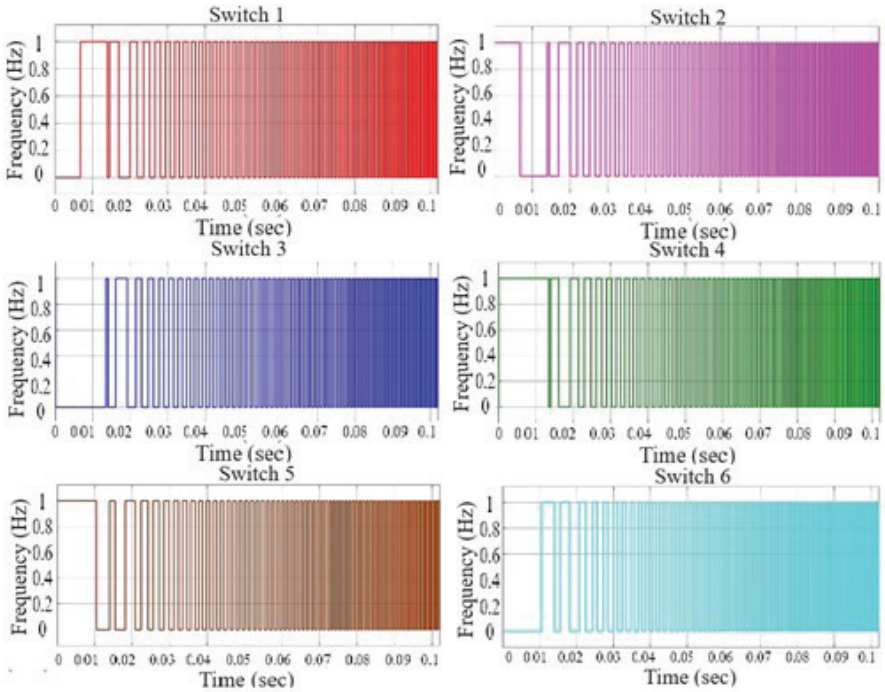

Figure 12: Switching signals of the proposed model.

The graph in Figure 12 illustrates the time-frequency characteristics of six switching devices (Switches 1 to 6) controlled by the ANN-based adaptive PWM mechanism over a 0.1-second simulation period. Each plot shows a progressive increase in switching frequency from approximately 0.1 Hz to nearly 1 Hz, demonstrating the adaptive learning behavior of the ANN controller. Switch one and Switch two show a steady rise in frequency, stabilizing close to 1 Hz around 0.08 seconds. Switches 3 and 4 exhibit a faster transition, reaching higher frequencies by 0.06 seconds, indicating a stronger compensation response. Switch 5 follows a smoother gradient, with a rise from 0.1 Hz to 0.8 Hz over the same time range. Switch six displays a slightly oscillatory pattern at the start but eventually stabilizes near 1 Hz, showing dynamic adaptation to load and grid conditions. The variation among all switches confirms that the ANN dynamically adjusts the PWM signals in real time based on system feedback, optimizing converter switching behavior for improved power quality and system stability.

3. With UPQC and Supercapacitor (SC)

http://dx.doi.org/10.21622/RESD.2025.11.2.1279

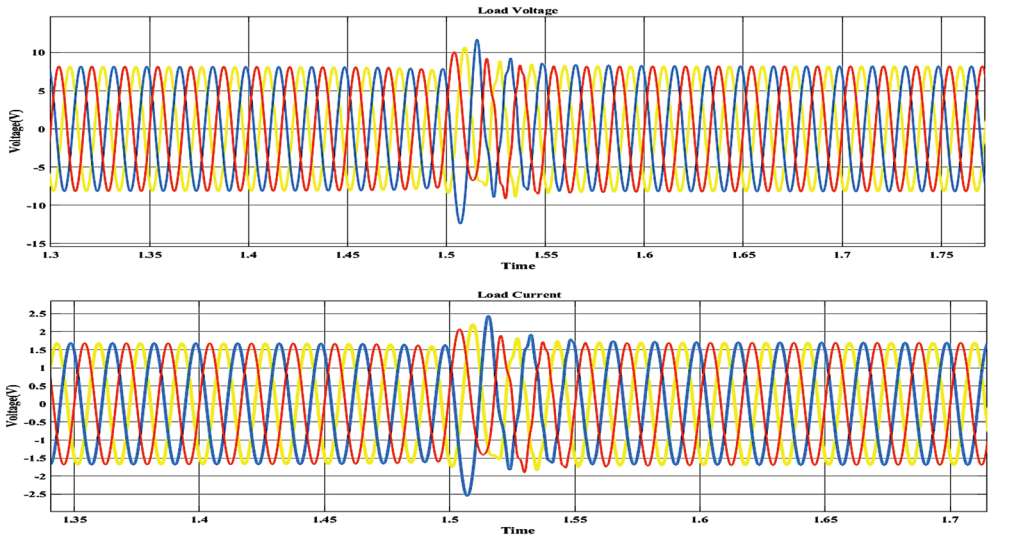

Figure 13: Comparison of voltage and current of DFIG without ANN.

Figure 13 displays the three-phase load voltage and current waveforms during a transient event under the control of the proposed system. In the load voltage graph, which shows the load voltage, the waveforms for the three phases (red, yellow, and blue) are initially balanced and sinusoidal with peak values around ±10 V. However, a noticeable disturbance occurs around 1.5 seconds, where one phase experiences a sharp voltage dip exceeding -12 V, followed by quick recovery. This indicates a voltage sag or disturbance that the system attempts to compensate for. Post-disturbance, the voltages return to stable sinusoidal waveforms, demonstrating the controller's ability to restore voltage quality. The load current graph shows the corresponding load current waveforms, which exhibit a similar behavior. Before the disturbance at 1.5 seconds, the currents are nearly sinusoidal with peak values of about ±2 A. During the disturbance, one phase experiences a sharp overshoot beyond +2.5 A and undershoot below -2.5 A, indicating the system's compensating current response. After the event, the currents return to balanced sinusoidal form, confirming effective transient compensation. Overall, the plots reflect the controller's rapid reaction to the disturbance and successful restoration of voltage and current quality.

4. With UPQC, SC, and ANN-Based PWM (Proposed SENCO Model)

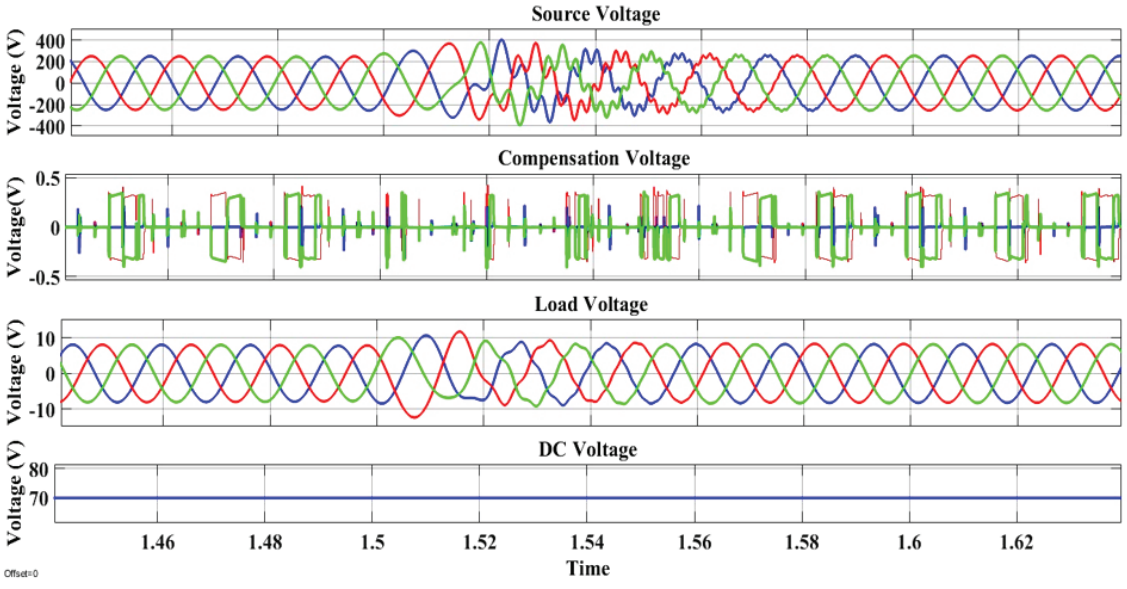

Figure 14: Voltage output of DFIG with UPQC for the proposed model.

Volume 11, Issue 2, December 2025 - ISSN 2356-8569
http://dx.doi.org/10.21622/RESD.2025.11.2.1279

The graph highlighted in Figure 14 shows a power system's behavior over a 0.1-second interval, focusing on source voltage, compensation voltage, load, and DC voltages. Source voltage exhibits a sinusoidal waveform, indicating a balanced AC supply. The compensation voltage remains close to 0.01 V, indicating no significant disturbances or neutralizing deviations to stabilize the system. The load voltage shows a sinusoidal waveform, but its magnitude is significantly reduced compared to the source voltage, indicating a step-down process or voltage regulation. The DC voltage remains constant at 70 V, demonstrating effective DC-link voltage regulation. This stability is crucial for systems using power electronic converters, ensuring consistent operation of downstream components. In summary, the graph demonstrates a well-regulated power system with sinusoidal and balanced source voltage, minimal compensation voltage, scaled load voltage, and constant DC voltage, demonstrating efficient voltage management and control.

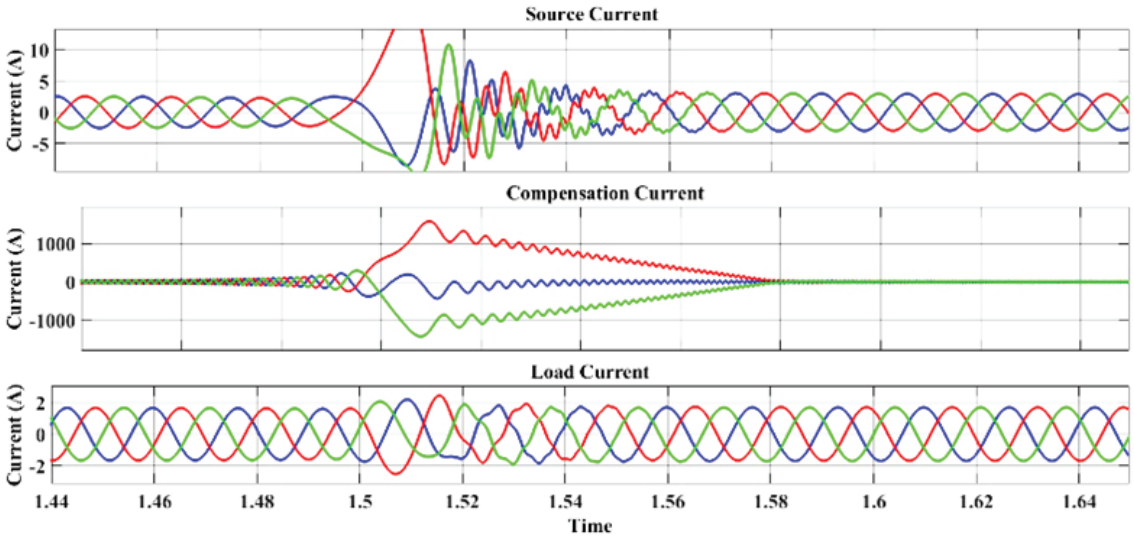

Figure 15: Current output of DFIG with UPQC for the proposed model.

Figure 15 illustrates the current behavior of the DFIG-based source, UPQC compensation unit, and the grid (load) during a 10-second simulation period. A nonlinear load disturbance is introduced between 1.48 s and 1.58 s. During this interval, the source (DFIG) current exhibits increased distortion due to the nonlinear characteristics of the load. The compensation current generated by the UPQC shows significant dynamic activity during this period, indicating its operation in mitigating the harmonic and transient components. The grid (load) current remains relatively smooth and stable, oscillating between approximately +2 A and −2 A, demonstrating the UPQC's effectiveness in isolating the load from source-side disturbances and preserving power quality during the nonlinear disturbance window.

http://dx.doi.org/10.21622/RESD.2025.11.2.1279

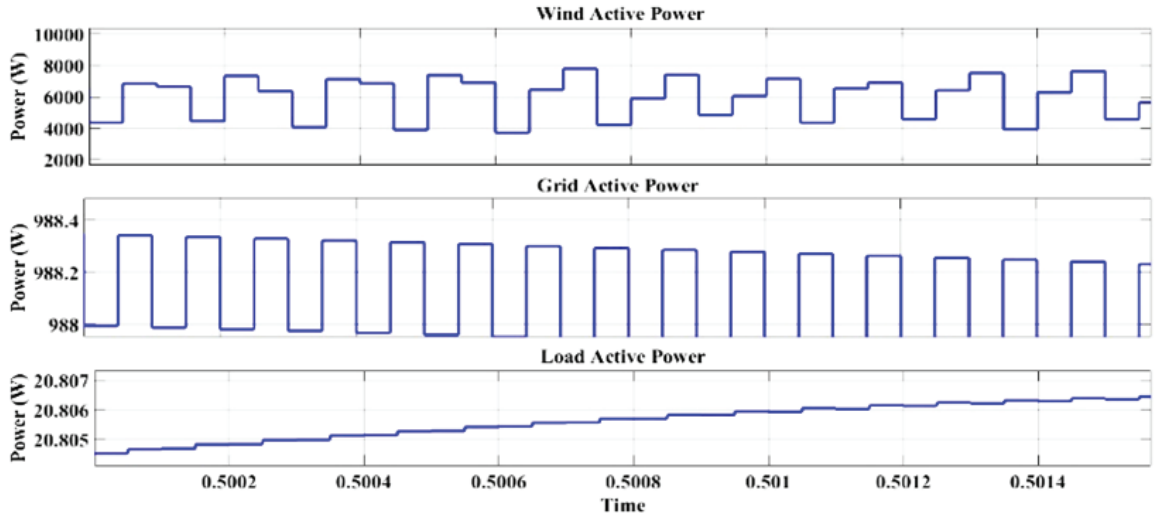

Figure 16: Active power outputs of DFIG with UPQC for the proposed model.

Figure 16 displays the active power profiles of the DFIG source, the grid (acting as the load), and the influence of nonlinear disturbance over time. The DFIG's active power shows periodic fluctuations between approximately -10^4 W and $+10^4$ W, reflecting the natural variability of wind generation. Between 1.48 s and 1.58 s, the interaction with the nonlinear load causes transient power deviations. The grid's active power response, oscillating between −4000 W and +8000 W, reflects the combined effect of power injection from the DFIG and compensation by the UPQC during the disturbance interval. In contrast, the load active power remains stable around 0–40 W, indicating that despite variations on the source side, the UPQC effectively ensures steady power delivery to the load, thereby maintaining grid-side power quality during the nonlinear disturbance period.

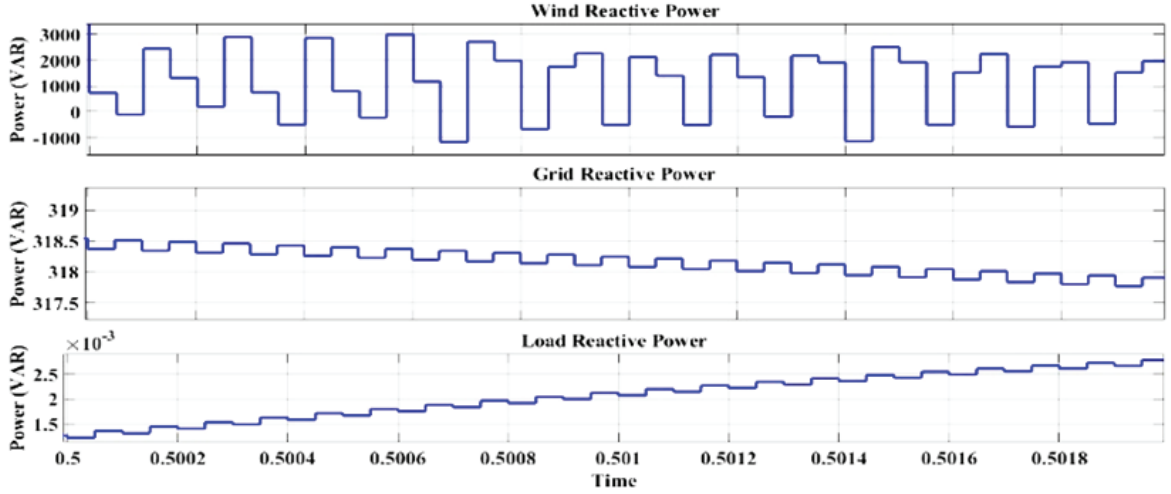

Figure 17: Reactive power outputs of DFIG with UPQC for the proposed model.

Figure 17 shows the wind system's reactive power shows significant variations, ranging from -10^5 VAR to $+10^5$ VAR. This reflects the reactive nature of wind power systems and their interaction with voltage and grid conditions. The grid reactive power displays smaller fluctuations compared to the wind system, ranging between −5000 VAR and +5000 VAR. This suggests the grid's stability in handling reactive power demand, ensuring voltage regulation and power factor correction. The load reactive power remains minimal, oscillating steadily around 0.2 VAR, representing consistent and balanced reactive power demand from the load. Despite these fluctuations, the grid maintains stability in handling

Volume 11, Issue 2, December 2025 - ISSN 2356-8569
http://dx.doi.org/10.21622/RESD.2025.11.2.1279

power disturbances, ensuring voltage regulation, and balancing reactive power. The load remains unaffected, with minimal variations in both active and reactive power, indicating consistent power delivery to meet demand.

D. THD comparison

The performance parameters, which compare the load and grid currents and voltages THD for DFIG with UPQC, are mentioned below.

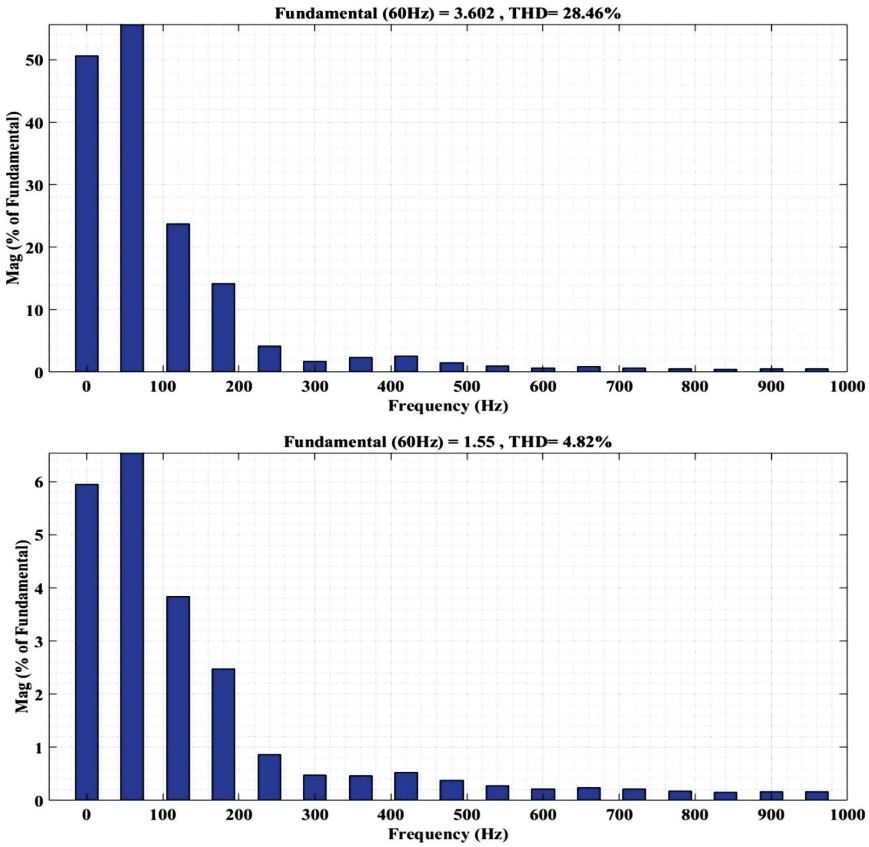

Figure 18: (a) Grid and (b) Load currents of THD.

The figure displayed in Figure 18 has two harmonic spectrums with their THD values. In the grid current, the fundamental frequency is again 60 Hz, but with a higher magnitude of 3.602% of the fundamental, and the THD is 28.46%, indicating significant distortion. Harmonics here exhibit larger amplitudes at 120 Hz; the magnitude is nearly 50%, while frequencies like 180 Hz and 240 Hz range between 20% and 10%. Beyond 600 Hz, the harmonic amplitudes decrease but remain notable. In load current, fundamental frequency is 60 Hz with a magnitude of 1.55% of the fundamental, and the THD is 4.82%, indicating low harmonic distortion. The harmonics show progressively decreasing amplitudes at 120 Hz, the magnitude is approximately 6%, at 180 Hz it is around 3%, and higher frequencies like 240 Hz and beyond have magnitudes below 1%, signifying a clean signal. The higher THD in the grid current indicates substantial waveform distortion, highlighting the need for harmonic compensation to ensure improved power quality.

http://dx.doi.org/10.21622/RESD.2025.11.2.1279

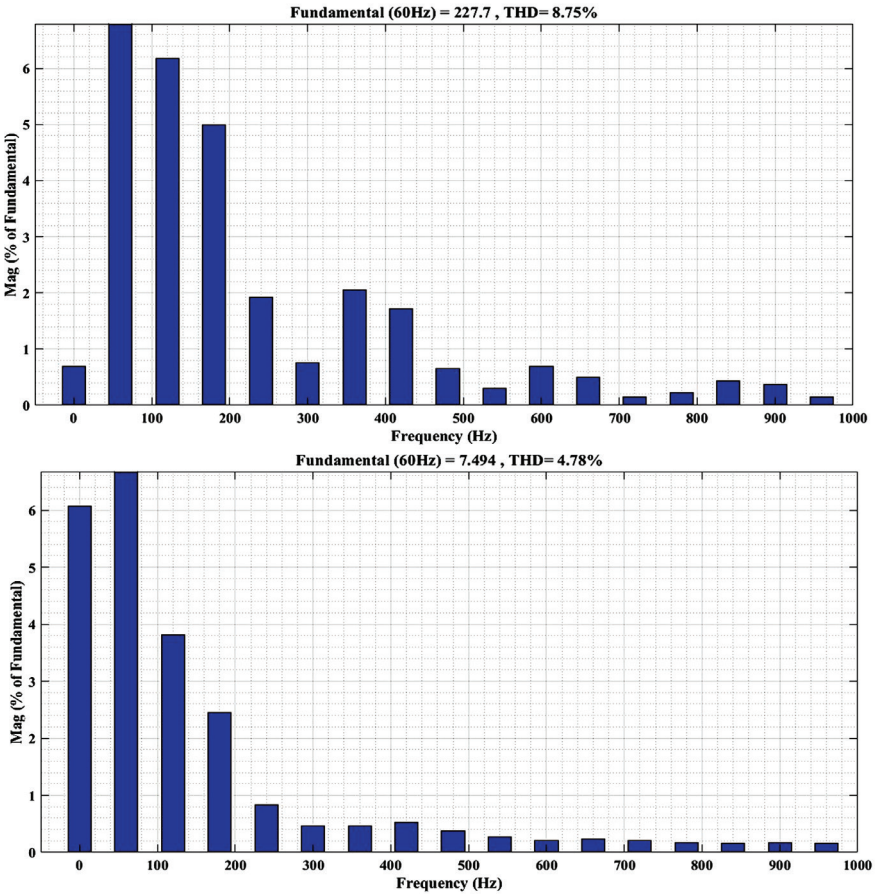

Figure 19: (a) Grid and (b) Load voltages of THD.

The graph in Figure 19 illustrates two harmonic spectrums with their respective THD values and frequency components for DFIG with UPQC. The grid voltage THD has the fundamental frequency of 60 Hz, with a much higher magnitude of 227.8% of the fundamental and a THD of 8.76%, indicating greater harmonic distortion. Here, the harmonics exhibit significant amplitudes, with values around 6% at 120 Hz, 5% at 180 Hz, and 3-4% at 240 Hz, 300 Hz, and 400 Hz, remaining evident even up to 1000 Hz. In the load voltage THD, the fundamental frequency is 60 Hz with a magnitude of 7.494% of the fundamental, and the THD is 4.77%, indicating relatively low distortion. The harmonics decrease in magnitude with values of approximately 6% at 120 Hz, 4% at 180 Hz, and below 2% for higher frequencies like 240 Hz, 300 Hz, and beyond, showing minimal impact from higher-order harmonics. On comparing both the voltages, the grid voltage has a higher THD, suggesting the need for improved harmonic filtering compared to the load voltage.

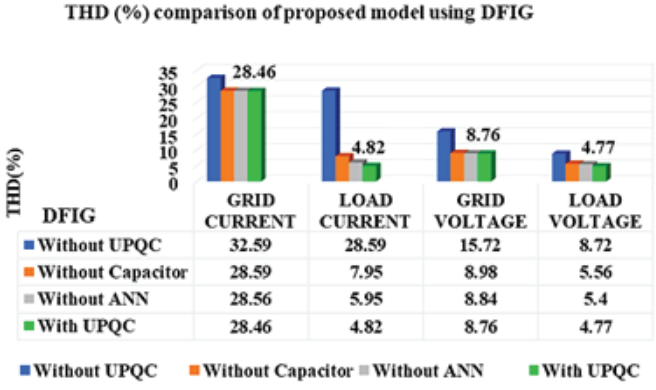

Figure 20: THD comparison for the proposed model using DFIG.

Volume 11, Issue 2, December 2025 - ISSN 2356-8569
http://dx.doi.org/10.21622/RESD.2025.11.2.1279

Figure 20 presents a comparative analysis of THD in grid and load parameters under various scenarios using the DFIG model, respectively. In the DFIG-based system, the highest THD occurs at 32.59% without UPQC, which is reduced to 28.59% without a capacitor and further to 28.46% with UPQC. Similarly, THD in load parameters decreases from 7.95% without a capacitor and 5.95% without ANN to 4.82% with UPQC, and for another scenario, from 15.72% without UPQC to 8.98% without a capacitor, 8.84% without ANN, and 8.76% with UPQC, highlighting the UPQC's effectiveness in enhancing power quality upon UPQC integration. These consistent reductions across both models confirm that the integration of UPQC significantly improves power quality by minimizing THD in grid and load currents and voltages, contributing to a more stable, reliable, and efficient power system, particularly in renewable energy applications.

E. Comparison of Proposed Method

The proposed SENCO method is compared with existing power quality enhancement techniques.

Table 5: Comparison of Proposed Method

Methods	ENERGY SOURCE	Source	Active power	Reactive power	Voltage THD	Current THD
[34]	Grid	-	✗	✓	✗	✓7%
[35]	Grid	Solar PV	✓	✗	~2%	✗3%
[36]	Grid and wind	DFIG	✓	✓	✗ (~7.7%)	✓ (~2%)
[37]	Hydro	PMSG	✗	✓	3.4-4%	4-5%
Proposed	Grid and wind	DFIG	✓	✓	4.78	4.82

Table 5 compares different power quality methods based on energy source and performance. Grid-only systems ([34], [35]) offer limited compensation with higher THD. Wind-based DFIG ([36]) improves compensation but suffers from voltage distortion. Hydro-PMSG ([37]) supports reactive power but lacks active compensation. The **proposed DFIG-based wind-grid method** provides both active and reactive power support with **better THD performance** (4.78% voltage, 4.82% current).

V. CONCLUSION

The integration of the UPQC significantly enhances system performance and power quality compared to configurations without it. The proposed SENCO model demonstrates its effectiveness in maintaining grid voltage stability at 400 V with minimal fluctuations and sustaining balanced load voltage at 200 V under various operating conditions. The UPQC effectively regulates grid current, limiting its peak to 10 A and rapidly suppressing disturbances using compensation currents reaching ±500 A. In contrast, the system without UPQC exhibits pronounced instability, with grid current spiking up to 20 A and no compensatory mechanism to restore balance, leading to distorted load currents and voltage fluctuations. Power quality analysis further supports the effectiveness of the UPQC. Without compensation, the grid current and voltage exhibit high THD values of 28.46% and 8.76%, respectively. With the UPQC in operation, these THDs are significantly reduced, and the load current and voltage THDs are maintained at low levels of 4.82% and 4.77%, respectively. While removing key elements such as the ANN, super capacitor, or UPQC has little impact on fundamental voltage and current levels, it results in persistently high harmonic distortion, especially on the grid side. The ANN-based adaptive control and super capacitor-enhanced support in the SENCO configuration enable fast and intelligent compensation under dynamic load and generation conditions. Overall, the proposed system ensures improved harmonic suppression, voltage stability, and reliable energy delivery, making it highly suitable for microgrids with nonlinear loads and renewable energy integration, such as wind power systems.

References

[1] M. Bajaj, S. Aggarwal, and A. K. Singh, "Power Quality Concerns with Integration of RESs into the Smart Power Grid and Associated Mitigation Techniques," in *2020 IEEE 9th Power India International Conference (PIICON)*, IEEE, Feb. 2020, pp. 1–6. doi: 10.1109/PIICON49524.2020.9113008.

[2] A. M. Abdallah, "Suppression of Power Quality Problems by using MPC-Based UPQC Technique," *ATBU Journal of Science, Technology and Education*, vol. 11, no. 1, pp. 40–59, 2023.

[3] O. P. Mahela, B. Khan, H. Haes Alhelou, and S. Tanwar, "Assessment of power quality in the utility grid integrated with wind energy generation," *IET Power Electronics*, vol. 13, no. 13, pp. 2917–2925, Oct. 2020, doi: 10.1049/iet-pel.2019.1351.

[4] B. S. Goud and B. L. Rao, "Power Quality Enhancement in Grid-Connected PV/Wind/Battery Using UPQC: Atom Search Optimization," *Journal of Electrical Engineering and Technology*, vol. 16, no. 2, 2021, doi: 10.1007/s42835-020-00644-x.

[5] M. H. Hassan, F. Daqaq, S. Kamel, A. G. Hussien, and H. M. Zawbaa, "An enhanced hunter-prey optimization for optimal power flow with FACTS devices and wind power integration," *IET Generation, Transmission and Distribution*, vol. 17, no. 14, 2023, doi: 10.1049/gtd2.12879.

[6] T. E. Rao, K. M. Tatikonda, S. Elango, and J. C. Kumar, "Power Quality Improvement in Microgrid System Using PSO-Based UPQC Controller," in *Microgrid Technologies*, 2021. doi: 10.1002/9781119710905.ch11.

[7] R. W. Kotla and S. R. Yarlagadda, "Real-time Simulations on Ultracapacitor based UPQC for the Power Quality Improvement in the Microgrid," *Journal of New Materials for Electrochemical Systems*, vol. 24, no. 3, 2021, doi: 10.14447/jnmes.v24i3.a04.

[8] P. Weber, "Novel Isolated Measurement System and Stochastic Modeling of Voltage Transients for Power Quality," Doctoral dissertation, Arizona State University, 2024.

[9] R. T. Moyo, M. Dewa, H. F. M. Romero, V. A. Gómez, J. I. M. Aragonés, and L. Hernández-Callejo, "An adaptive neuro-fuzzy inference scheme for defect detection and classification of solar PV cells," *Renewable Energy and Sustainable Development*, vol. 10, no. 2, p. 218, Sep. 2024, doi: 10.21622/resd.2024.10.2.929.

[10] K. Srilakshmi *et al.*, "Optimization of ANFIS controller for solar/battery sources fed UPQC using an hybrid algorithm," *Electrical Engineering*, vol. 106, no. 4, 2024, doi: 10.1007/s00202-023-02185-8.

[11] S. Kinga, T. F. Megahed, H. Kanaya, and D.-E. A. Mansour, "Enhancing robustness and control performance of voltage source inverters using Kalman filter adaptive observer and ANN-based model predictive controller," *Neural Comput Appl*, vol. 36, no. 33, pp. 21073–21090, 2024.

[12] S. K. Yadav, K. B. Yadav, and A. Priyadarshi, "Performance analysis of three-phase solar PV, BESS, and Wind integrated UPQC for power quality improvement," *Computers and Electrical Engineering*, vol. 116, p. 109230, May 2024, doi: 10.1016/j.compeleceng.2024.109230.

[13] G. Wang, Z. Wu, and Z. Liu, "Predictive direct control strategy of unified power quality conditioner based on power angle control," *International Journal of Electrical Power and Energy Systems*, vol. 156, 2024, doi: 10.1016/j.ijepes.2023.109718.

[14] S. Das, H. M. Ishrak, M. M. Hasan, and M. A. Kabir, "Empirical analysis of power quality using UPQC with hybrid control techniques," *Results in Engineering*, vol. 20, 2023, doi: 10.1016/j.rineng.2023.101527.

[15] T. Lei, S. Riaz, N. Zanib, M. Batool, F. Pan, and S. Zhang, "Performance Analysis of Grid-Connected Distributed Generation System Integrating a Hybrid Wind-PV Farm Using UPQC," *Complexity*, vol. 2022, 2022, doi: 10.1155/2022/4572145.

[16] S. S. Dheeban and N. B. Muthu Selvan, "ANFIS-based Power Quality Improvement by Photovoltaic Integrated UPQC at Distribution System," *IETE J Res*, vol. 69, no. 5, 2023, doi: 10.1080/03772063.2021.1888325.

[17] K. Srilakshmi *et al.*, "Optimal design of solar/wind/battery and EV fed UPQC for power quality and power flow management using enhanced most valuable player algorithm," *Front Energy Res*, vol. 11, 2023, doi: 10.3389/fenrg.2023.1342085.

[18] M. Pushkarna *et al.*, "A new-fangled connection of UPQC tailored power device from wind farm to weak-grid," *Front Energy Res*, vol. 12, 2024, doi: 10.3389/fenrg.2024.1355867.

[19] J. X. Jin, R. H. Yang, R. T. Zhang, Y. J. Fan, Q. Xie, and X. Y. Chen, "Combined low voltage ride through and power smoothing control for DFIG/PMSG hybrid wind energy conversion system employing a SMES-based AC-DC unified power quality conditioner," *International Journal of Electrical Power and Energy Systems*, vol. 128, 2021, doi: 10.1016/j.ijepes.2020.106733.

[20] H. Mahar *et al.*, "Implementation of ANN Controller Based UPQC Integrated with Microgrid," *Mathematics*, vol. 10, no. 12, p. 1989, Jun. 2022, doi: 10.3390/math10121989.

[21] M. Sivakumar, P. Kannan, and S. Chenthur Pandian, "Mitigation of PQ Issues Using an Enhanced UPQC-Based ANN Approach," *Journal of Circuits, Systems and Computers*, vol. 28, no. 3, 2019, doi: 10.1142/S0218126619500464.

[22] R. Yang, J. Jin, Q. Zhou, S. Mu, and A. Abu-Siada, "Superconducting Magnetic Energy Storage Based DC Unified Power Quality Conditioner with Advanced Dual Control for DC-DFIG," *Journal of Modern Power Systems and Clean Energy*, vol. 10, no. 5, 2022, doi: 10.35833/MPCE.2021.000354.

[23] R. W. Kotla and S. R. Yarlagadda, "Real-time Simulations on Ultracapacitor based UPQC for the Power Quality Improvement in the Microgrid," *Journal of New Materials for Electrochemical Systems*, vol. 24, no. 3, pp. 166–174, Sep. 2021, doi: 10.14447/jnmes.v24i3.a04.

[24] M. K. Döşoğlu, "Enhancement of LVRT Capability in DFIG-Based Wind Turbines with STATCOM and Supercapacitor," *Sustainability (Switzerland)*, vol. 15, no. 3, 2023, doi: 10.3390/su15032529.

[25] M. M. Afzal *et al.*, "A comparative study of supercapacitor-based STATCOM in a grid-connected photovoltaic system for regulating power quality issues," *Sustainability (Switzerland)*, vol. 12, no. 17, 2020, doi: 10.3390/SU12176781.

[26] N. Samala and C. Bethi, "Harnessing synergy: a holistic review of hybrid renewable energy systems and unified power quality conditioner integration," *Journal of Electrical Systems and Information Technology*, vol. 12, no. 1, p. 4, 2025.

[27] L. Qu and W. Qiao, "Constant power control of DFIG wind turbines with supercapacitor energy storage," *IEEE Trans Ind Appl*, vol. 47, no. 1, 2011, doi: 10.1109/TIA.2010.2090932.

[28] S. Kumar, R. Agarwal, and H. Subhadra, "Adaptive bayesian sparse polynomial chaos expansion for voltage balance of an isolated microgrid at peak load," *Renewable Energy and Sustainable Development*, vol. 11, no. 1, p. 161, Jun. 2025, doi: 10.21622/resd.2025.11.1.1281.

[29] M. Q. Duong, F. Grimaccia, S. Leva, M. Mussetta, G. Sava, and S. Costinas, "Performance analysis of grid-connected wind turbines," Scientific Bulletin-" Politehnica," *University Of Bucharest Series C Electrical Engineering And Computer Science*, vol. 74, no. 4, pp. 169–180, 2014.

[30] P. Ebiarede and A. F. Okilo, "Minimization of Total Harmonic Distortion Introduced by Distributed Generation in a Distribution Network using Unified Power Quality Conditioner," *FUPRE Journal of Scientific and Industrial Research (FJSIR)*, vol. 6, no. 3, pp. 12–25, 2022.

[31] A. Y. Qasim, F. R. Tahir, and A. N. B. Alsammak, "Improving Power Quality in Distribution Systems Using UPQC: An Overview," *Journal Européen des Systèmes Automatisés*, vol. 57, no. 2, pp. 311–322, Apr. 2024, doi: 10.18280/jesa.570201.

[32] P. Singh, N. K. Singh, and A. K. Singh, "Intelligent hybrid method to predict generated power of solar PV system," *Renewable Energy and Sustainable Development*, vol. 11, no. 1, p. 141, May 2025, doi: 10.21622/resd.2025.11.1.1264.

[33] H. Mahar *et al.*, "Implementation of ANN Controller Based UPQC Integrated with Microgrid," *Mathematics*, vol. 10, no. 12, p. 1989, Jun. 2022, doi: 10.3390/math10121989.

[34] C.-S. Lam, L. Wang, S.-I. Ho, and M.-C. Wong, "Adaptive Thyristor-Controlled LC-Hybrid Active Power Filter for Reactive Power and Current Harmonics Compensation With Switching Loss Reduction," *IEEE Trans Power Electron*, vol. 32, no. 10, pp. 7577–7590, Oct. 2017, doi: 10.1109/TPEL.2016.2640304.

[35] M. Golla, S. Thangavel, S. P. Simon, and N. P. Padhy, "A Novel Control Scheme Using UAPF in an Integrated PV Grid-Tied System," *IEEE Transactions on Power Delivery*, vol. 38, no. 1, 2023, doi: 10.1109/TPWRD.2022.3180681.

[36] G. S. Chawda and A. G. Shaik, "Power quality improvement in rural grid using adaptive control algorithm to enhance wind energy penetration levels," *IEEE Trans. Smart Grid*, vol. 14, no. 3, pp. 2075–2084, 2023.

[37] C. D. Sanjenbam and B. Singh, "Modified Adaptive Filter Based UPQC for Battery Supported Hydro Driven PMSG System," *IEEE Trans Industr Inform*, vol. 19, no. 7, 2023, doi: 10.1109/TII.2022.3215950.